Hypersonic Vehicle (HSV) Modeling

U of M Faculty: Carlos Cesnik (PI), Jim Driscoll

Graduate students: Derek Dalle, Nathan Falkiewicz, Torstens Skujins, Nathan Scholten, Sean Torrez, Scott Frendreis, Matt Fotia

AFRL collaborators: Mike Bolender,

David Doman (team leader), Mike Oppenheimer

OSU collaborators: Jack McNamara, Andrea Serrani, and respective students

Overview

- Challenge: strong interactions among aerodynamics, elastic airframe and control effector deformations, heat transfer, and propulsion system (itself tightly integrated into the lifting body)
- Focus in two main areas:
  - Understanding the fundamental dynamics that must be retained in simple (low-order) control models (for design and evaluation) that can characterize the main aerothermoelastic effects coupled with propulsion in a 6-rigid DOF flight dynamics simulation of HSV; and
  - Study how to appropriately modify vehicle configuration to improve its dynamic controllability without compromising vehicle performance.
- All done in close collaboration with AFRL/RBCA researchers who will provide primarily the control design expertise as part of the Collaborative Center.

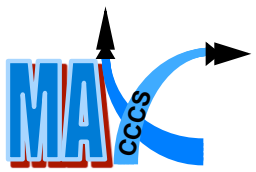

Introduction

- "Current" Control-Oriented Hypersonic Vehicle Models
  - Bolender, Doman, Oppenheimer and Co. open source simulink model
  - Mirmirani et al. model
- "Ground-Up" Modeling Approach
- Modeling Features:
  - 2-D longitudinal flight dynamics
  - Rigid control surfaces
  - Flexible states modeled using a beam
  - Thermo-elastic structure modeled using a beam
  - 1-D heating effects (through thickness) for material property degradation
  - Aerodynamics based on classical 2-D approximations or CFD table look-up
  - Propulsion system modeled using 1-D flow with heat addition

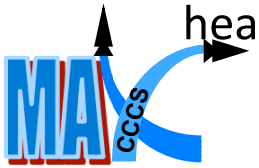

What about lateral and roll dynamics?

What about CS aerothermoelasticity?

What about lateral and torsional structural dynamics?

What about actual internal structural and component layout?

What about lengthwise distribution and effect of thermal stresses?

What about 3-D Flow, real gas effects, viscosity, aerodynamic damping, flow fidelity?

What about unmodeled engine dynamics?

Introduction

- Previous efforts have not adequately assessed model quality
- Hypersonic vehicles are high energy systems
  - Small errors can lead to catastrophic failures
  - Failures occur rapidly
- Natural questions:
  1. What level of modeling is good enough in the context of control?
  2. What is the uncertainty associated with the chosen level of fidelity?
- Ground testing of scaled comprehensive vehicle models not practical
- "High fidelity" comprehensive models required to answer these questions
  - Systematically validate FMs and ROMs
  - Identify appropriate fidelity
  - Uncertainty Characterization
  - "top-down" control oriented models

Coupling → Errors build with flight time

How does system couplings affect these answers?

Added Benefit: Advance state-of-the-art in other disciplines

Challenge: SOA in other disciplines not ready for direct creation of ROMS

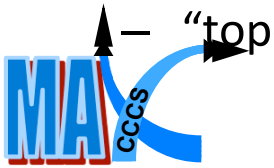

Leverage: NASA Hypersonic NRA

- Ohio State University/Univ. of Michigan team was awarded (Jan '08) a 3-year NASA NRA in Hypersonic Modeling for Control Design and Evaluation
  - NASA POC: Peter Ouzts (PM) and Don Soloway (API GNC)
  - Brought additional modeling and control expertise to the team:
    - Peretz Friedmann (UM): uncertainty characterization and aerothermoelasticity
    - Jack McNamara (OSU-PI): aerothermoelasticity
    - Andrea Serrani (OSU): nonlinear and robust control, control modeling and design
  - Five more students added to the HSV activities (plus some additional leveraged students)

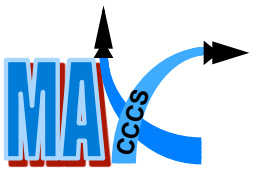

Flight Dynamics and Control Analysis

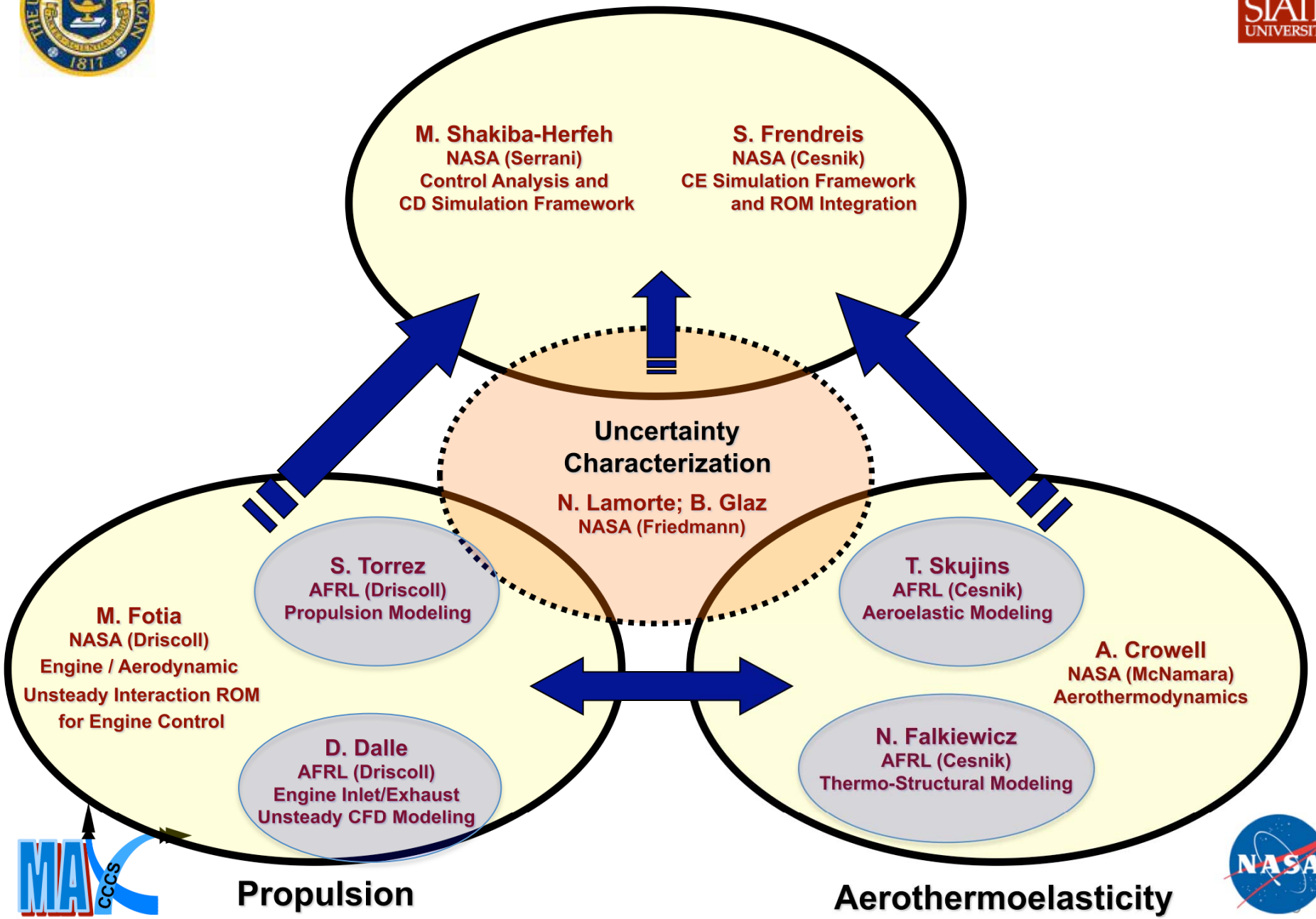

“Top-Down” Modeling Approach

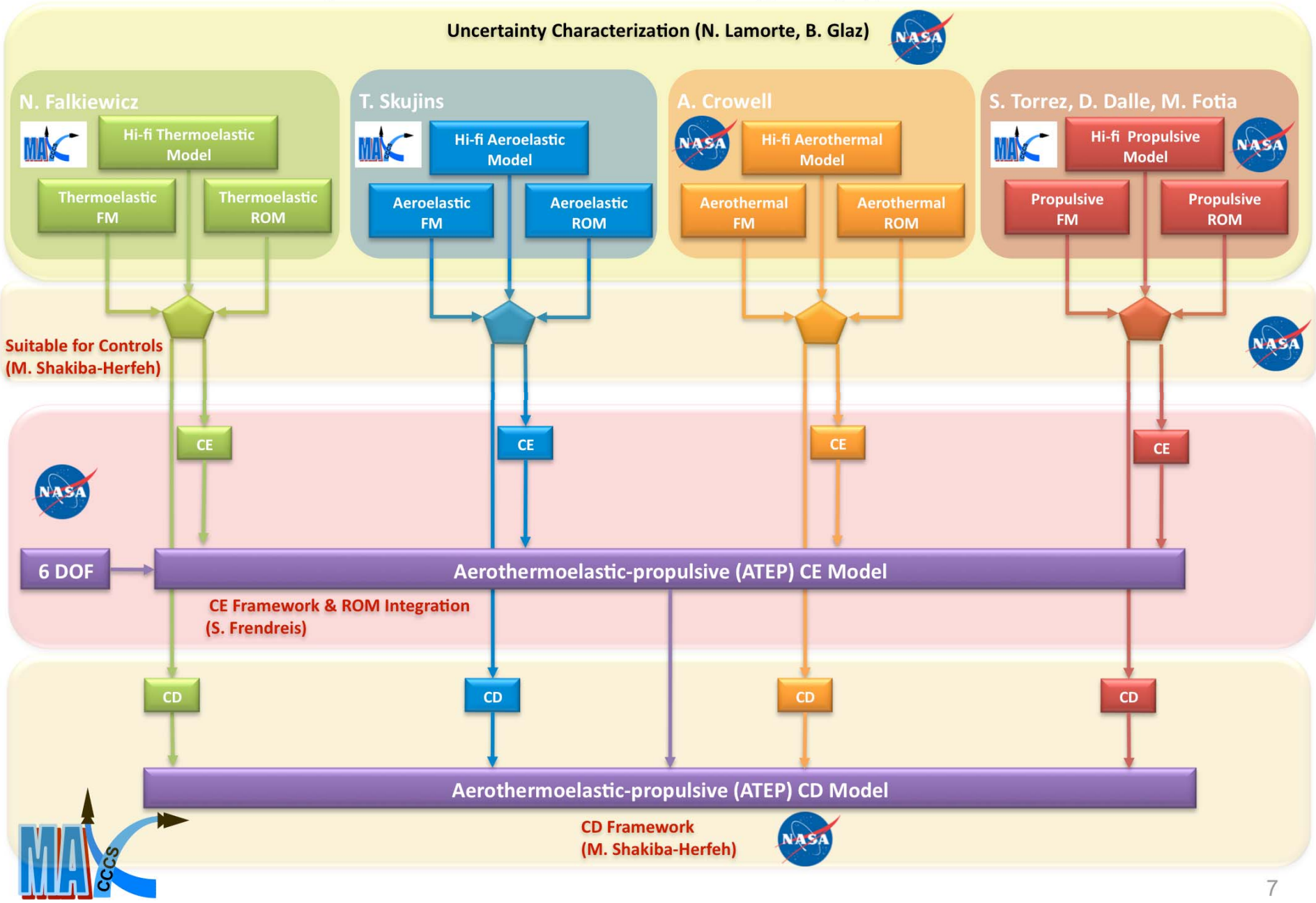

Issues Being Addressed in Collaborative Research

- Previous Model Features:
  - 2-D longitudinal flight dynamics
  - Rigid control surfaces
  - Flexible states modeled using a beam (transverse direction only)
  - Thermo-elastic structure modeled using a beam
  - 1-D heating effects (through thickness) for material property degradation
  - Aerodynamics based on classical 2-D approximations or CFD table look-up
  - Propulsion system modeled using 1-D flow with heat addition

- Enhanced Model Features:
  - 6 DOF flight dynamics
  - Flexible control surfaces
  - Flexible states modeled using a 3-D beam or modal representation
  - Representative Thermo-elastic structure
  - 3-D heating effects for material property degradation and thermal stresses
  - 3-D unsteady Aerothermodynamics
  - Propulsion model accounting for: dissociation, isolator shock losses, finite rate chemistry, efficiency factors, engine dynamics

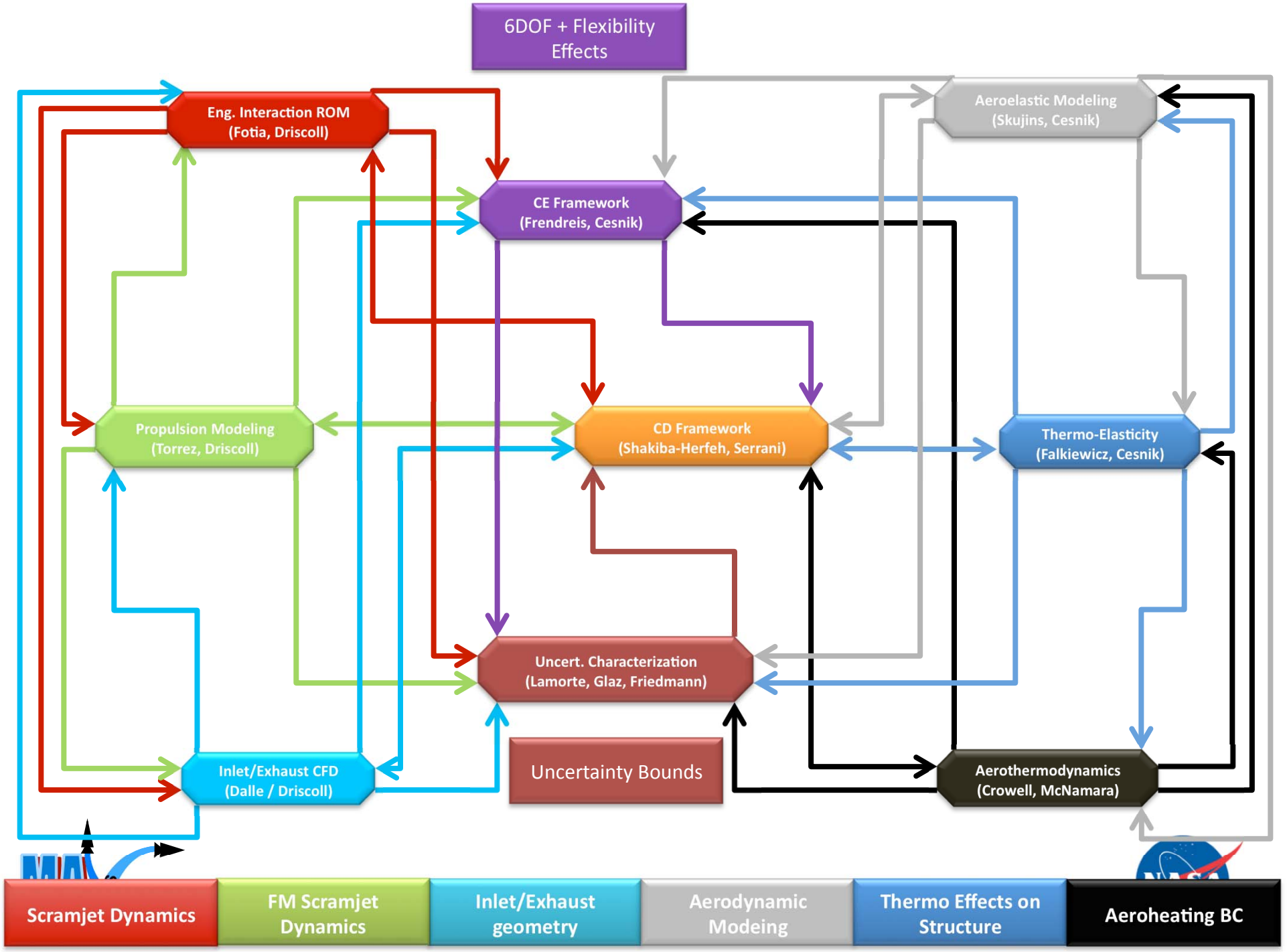
6DOF + Flexibility Effects
Eng. Interaction ROM (Fotia, Driscoll)
Aeroelastic Modeling (Skujins, Cesnik)
CE Framework (Frendreis, Cesnik)
Propulsion Modeling (Torrez, Driscoll)
CD Framework (Shakiba-Herfeh, Serrani)
Thermo-Elasticity (Falkiewicz, Cesnik)
Uncert. Characterization (Lamorte, Glaz, Friedmann)
Inlet/Exhaust CFD (Dalle / Driscoll)
Uncertainty Bounds
Aerothermodynamics (Crowell, McNamara)
Scramjet Dynamics
FM Scramjet Dynamics
Inlet/Exhaust geometry
Aerodynamic Modeing
Thermo Effects on Structure
Aeroheating BC

Different Interactions within MAX

Mid-year review Cesnik, Bolender, Driscoll, Doman, Falkiewicz, Fotia, Frendreis, McNamara, Oppenheimer, Serrani, Skujins, Scholtan, Torrez

Student summer at AFRL: Falkiewicz

Several day-visits to AFRL: Cesnik, Driscoll

AFRL visits to UM: Bolender, Doman, Oppenheimer

Meetings held at GNC conference: Bolender, Driscoll, Doman, Falkiewicz, Oppenheimer, Skujins, Torrez

Co-authoring several technical papers + submissions to journal paper/conferences in 2010

Technical interactions with McNamara and Serrani (OSU)

Flight Dynamics and Control Analysis

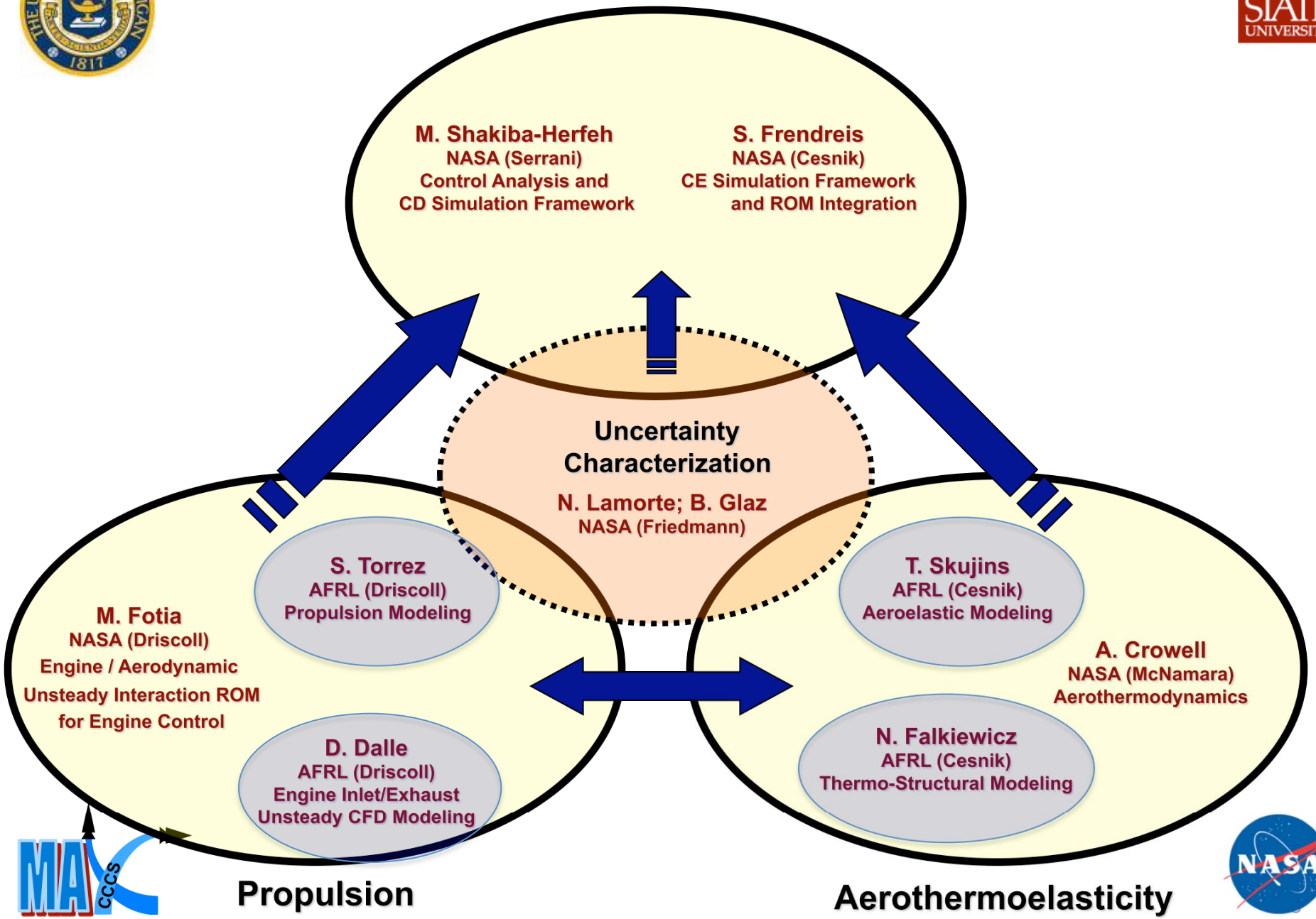

A Simplified Formulation of Aerodynamic Loads on a Three-Dimensional Hypersonic Vehicle

Torstens Skujins
Carlos E.S. Cesnik
Aerospace Engineering Department
University of Michigan, Ann Arbor

Michigan AFRL Collaborative Center in Control Sciences
Ann Arbor, MI, September 23-24 2009

Task Overview

- **Torstens Skujins (AFRL, Cesnik)** - Aeroelastic modeling of HSV and its control surfaces
  - Investigate fundamental aeroelastic models:
    - Extended (longitudinal + lateral) oblique shock/expansion aerodynamics modeling
    - Augment steady aero model with (unsteady) piston theory
    - Extended AFRL fundamental model for structural dynamics of the vehicle based on 3D beam model and 3D modal representations
  - Use CFD tools to model and investigate hypersonic vehicle unsteady aerodynamics
    - High-fidelity reference unsteady aerodynamic model for both 2D and 3D HSV representations
    - ROM based on Volterra series
  - Variable-fidelity aeroelastic models for aeroelasticity CD and CE representations

Agenda

- ***Overall approach***
- Top and bottom surface formulations
- Side surface formulation
- Summary and future work

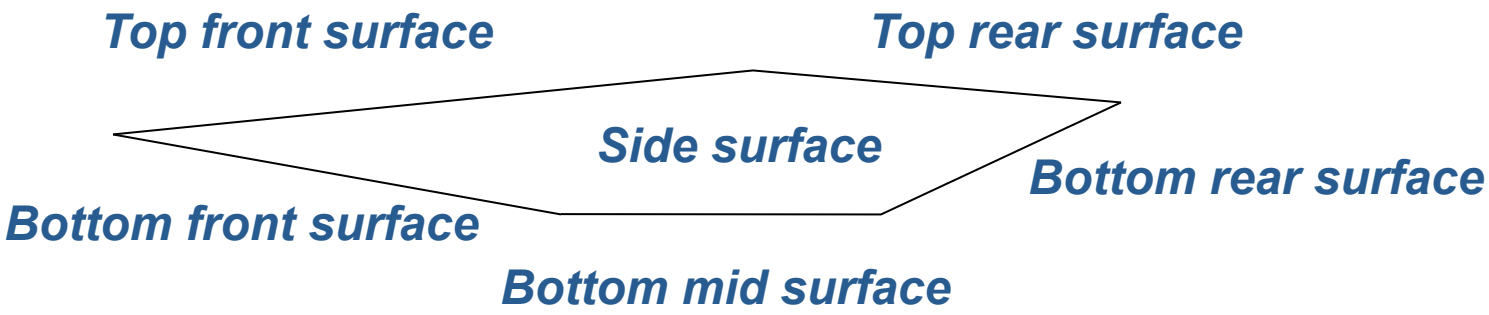

Current Hypersonic Vehicle Model

- 2-D model from Bolender and Doman (AFRL)[1] developed to study vehicle flight dynamics and evaluate control algorithms over a range of flight conditions
- Pressure and other flow properties on each surface calculated using 2-D shock/expansion fan equations

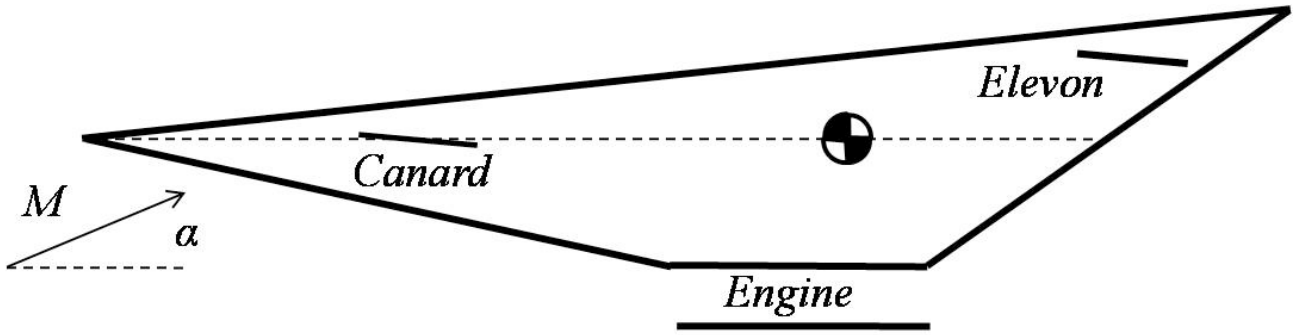

1. Bolender, M.A. and Doman, D.B., "Nonlinear Longitudinal Dynamical Model of an Air-Breathing Hypersonic Vehicle," *Journal of Spacecraft and Rockets*, Vol. 44, No. 2, 2007, p. 374-387

Model Extension

- Model currently being extended from 2-D to 3-D
- Many phenomena are 3-D and cannot be captured by 2-D model
- 3-D computations are too costly: relatively coarse 3-D HSV model steady simulation in CFD++ takes ~15 hours
- Reduced-order and/or simplified models a necessity
- Two step model extension approach:
  - 3-D extrusion of current 2-D model
  - Fully 3-D model

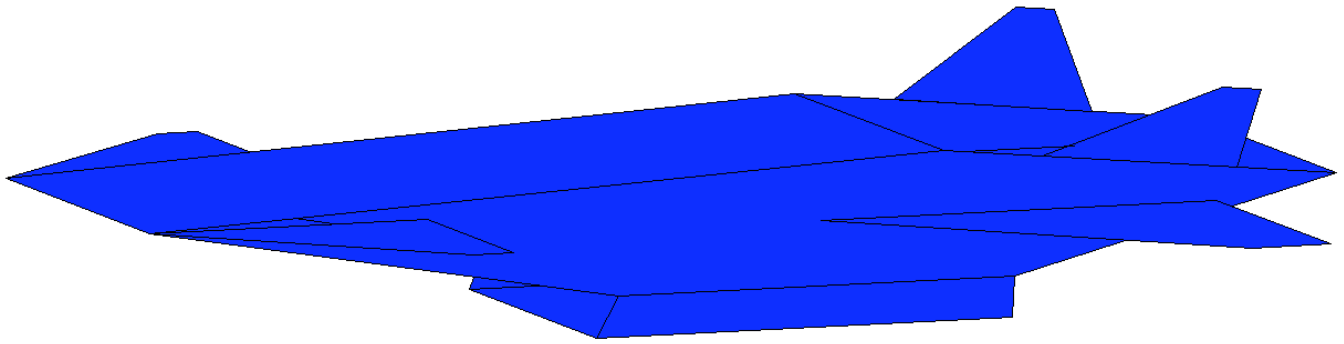

3-D FM Aerodynamic Approach

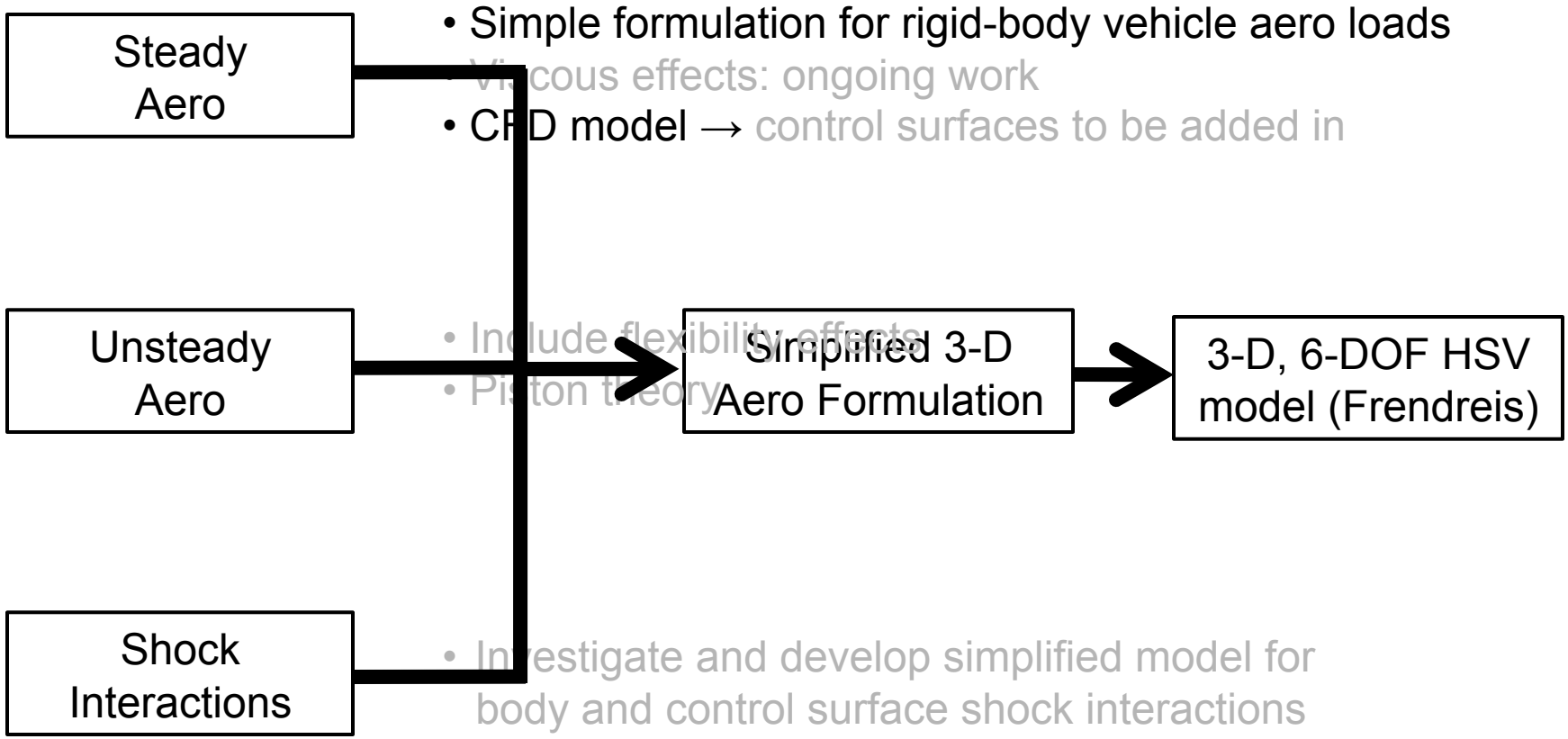

CFD Runs

- Inviscid CFD runs conducted using Metacomp's CFD++ 6.5.1
- Used to validate results of steady simplified aerodynamic model
- Unstructured mesh, ~2 million grid points
- Resultant forces and moments within 1% of those calculated with grid of 4 times as many points
- Both ANSYS ICEM CFD and Fluent's Gambit used to generate mesh, depending on specific case

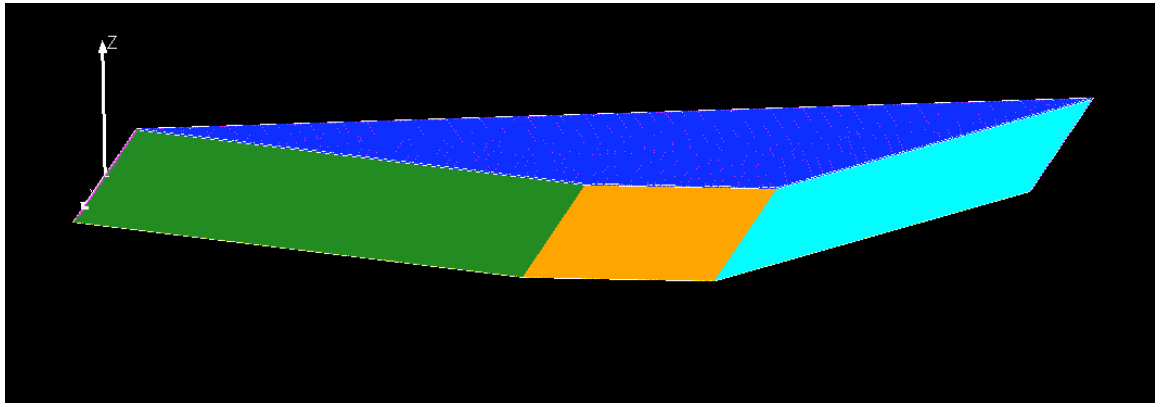

Agenda

- Overall approach
- ***Top and bottom surface formulations***
- Side surface formulation
- Summary and future work

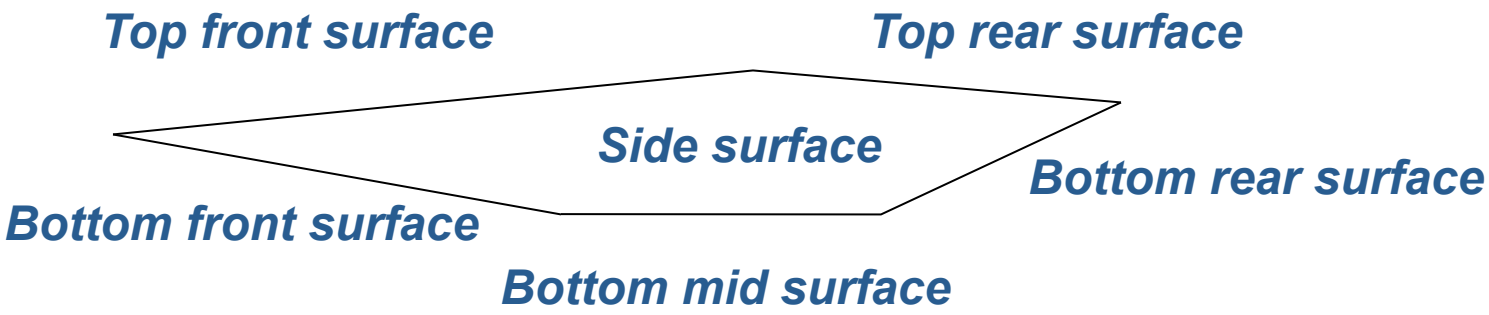

Sample Vehicle Geometry

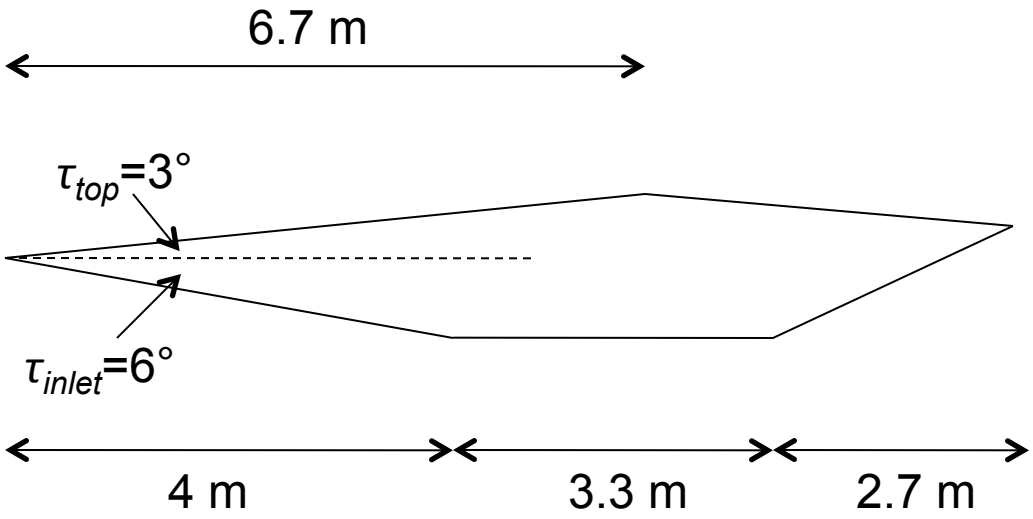

Side View

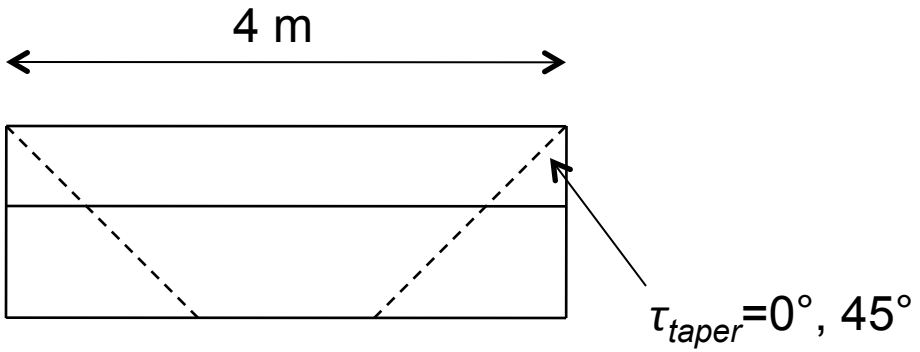

Front View

Front Surface Formulation Overview

- Flow in middle of surface not affected by edges
- Mach angle μ: maximum angle at which information can propagate downstream in supersonic flow; determines zone of influence of longitudinal boundaries

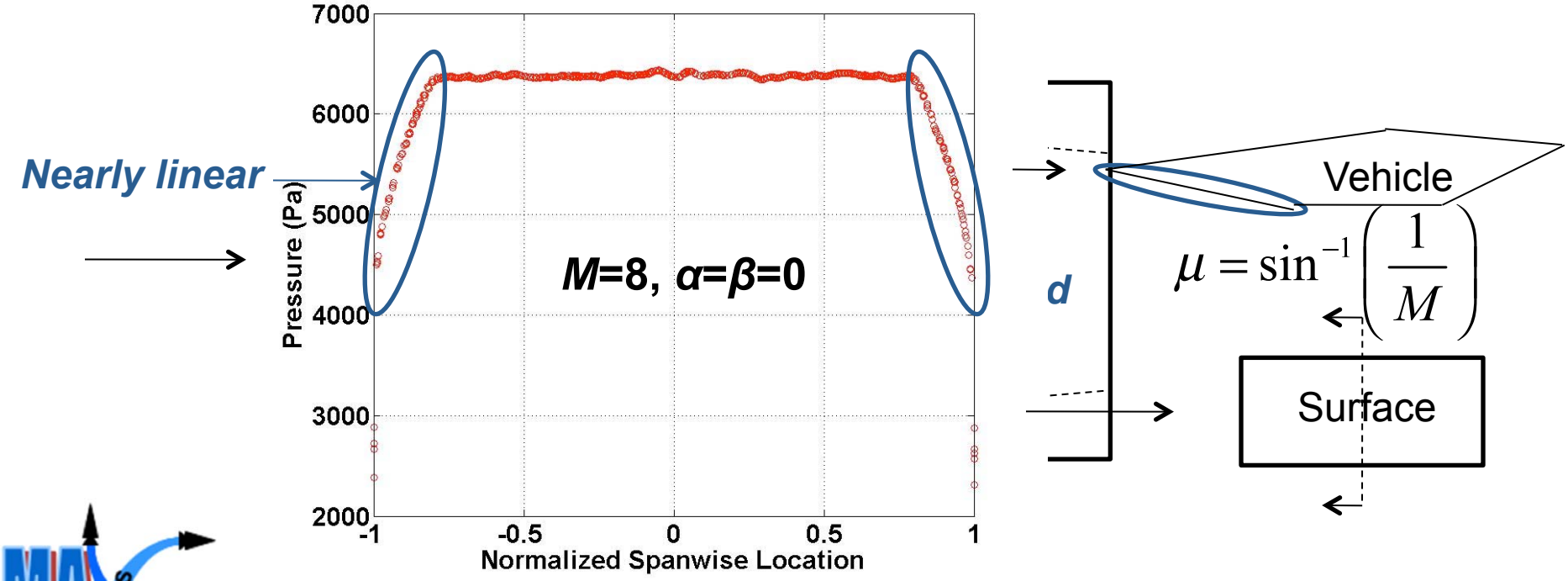

Pressure Distribution Calculation Summary

- 2-D shock/expansion equations used for areas not in the Mach cone regions
- Longitudinal boundary conditions found using Taylor-Maccoll conical flow equations[1] with wedge angle used as cone angle
  - Differential equation with freestream Mach number M_∞ and cone half-angle θ as variables
  - Wedge angle of surface with freestream flow is used as θ in formulation

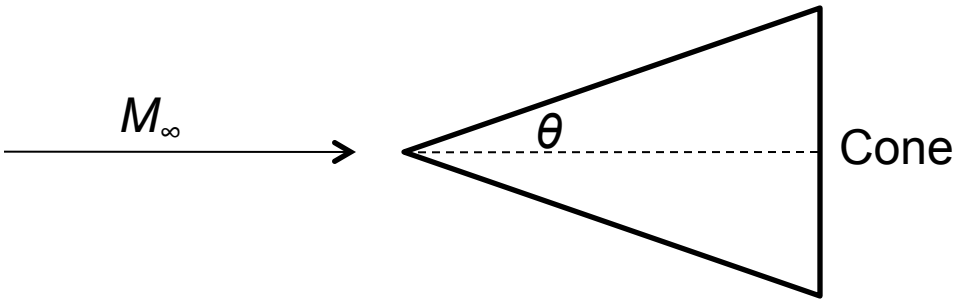

- Linearly interpolate between boundary conditions and 2-D flow conditions in the middle of the surface

1. Starkey, R.P. and Lewis, M.J., "A Shock-Expansion Method for Determining Surface Properties On Irregular Geometries," *Proceedings of the 40th Aerospace Sciences Meeting & Exhibit*, AIAA Paper No. 2002-0547, January 2002

Front Surface Pressure Comparisons: Mid-Surface Cut

M=8, α=β=0

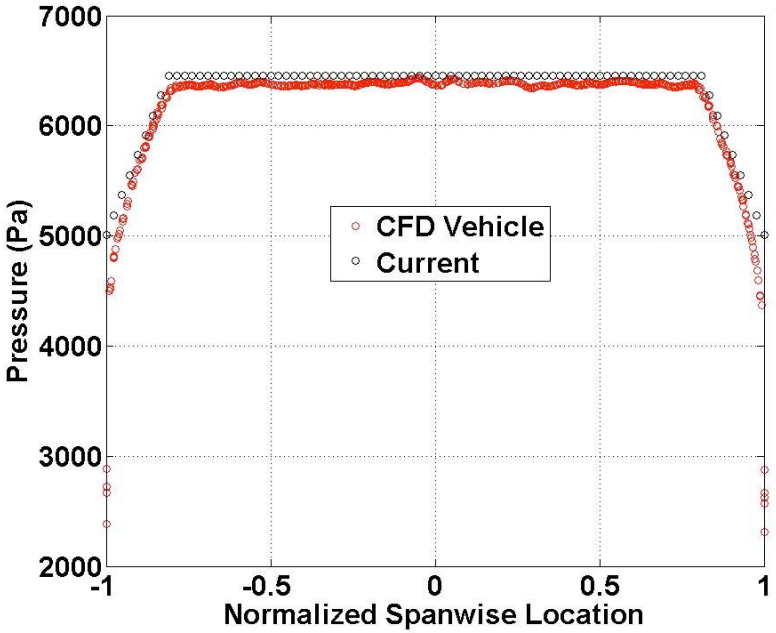

M=8, α=β=3˚

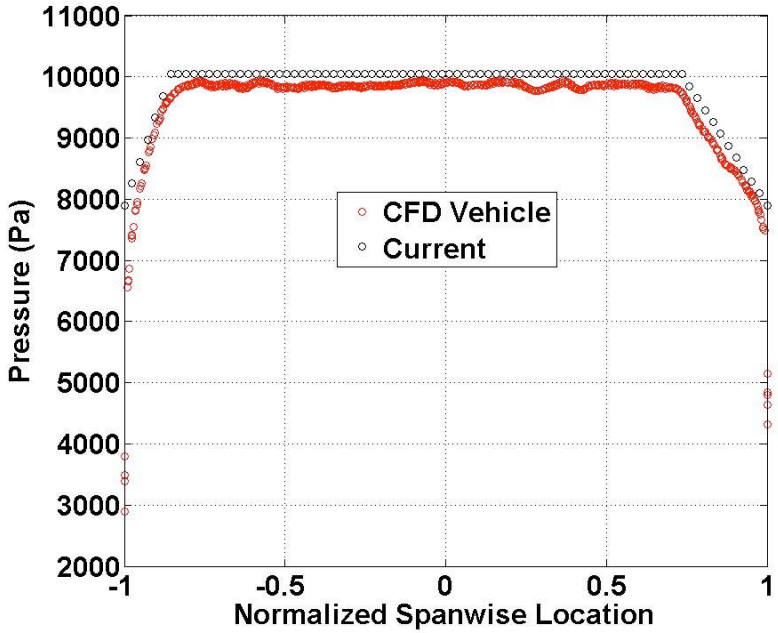

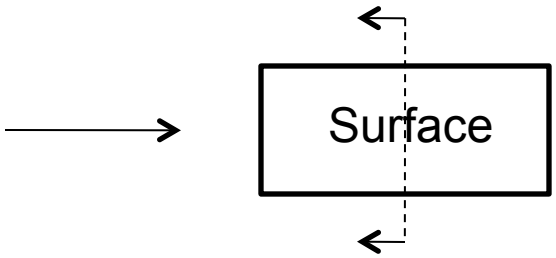

Good agreement with CFD data

Front Surface Pressure Comparisons: Trailing Edge Cut

M=8, α=β=0

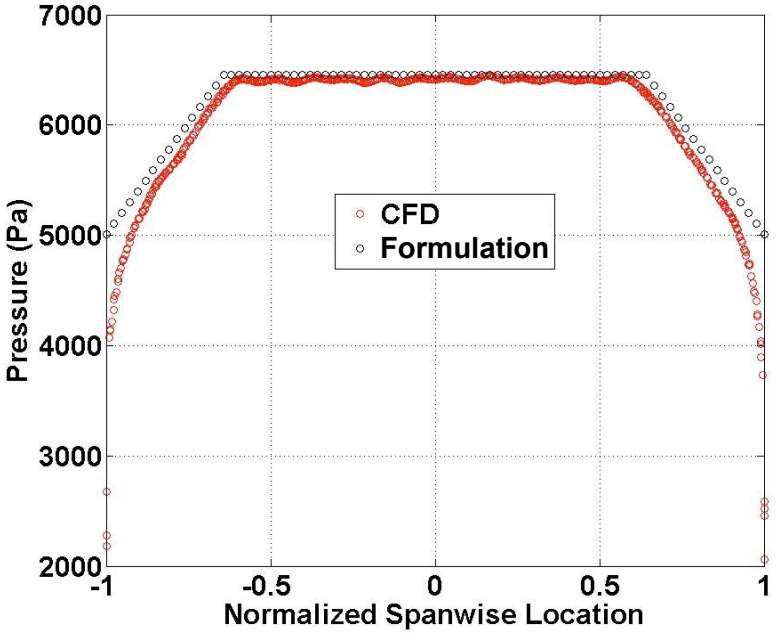

M=8, α=β=3˚

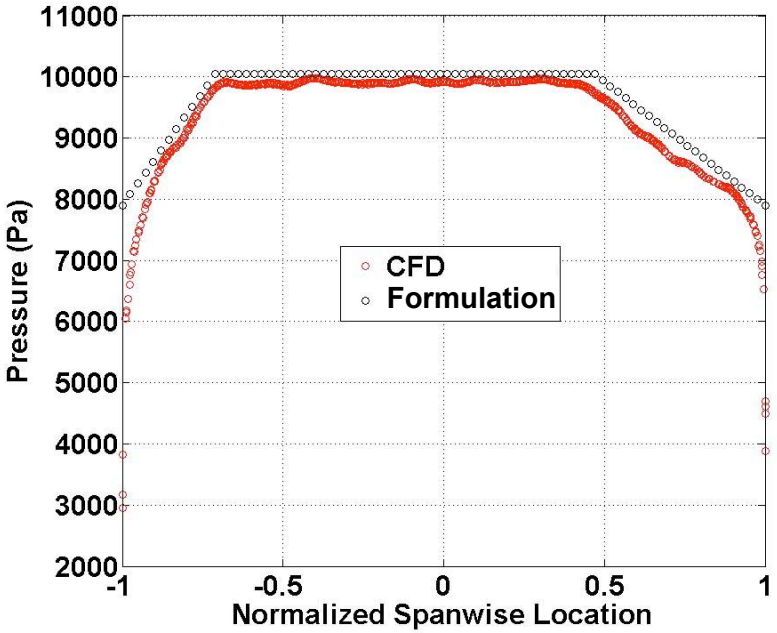

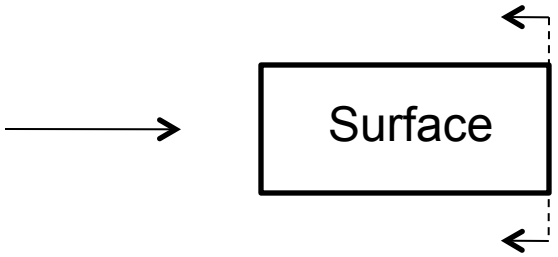

Good agreement with CFD data along entire length of surface

Front Surface Pressure Comparisons: Longitudinal Cut

M=8, α=β=3˚

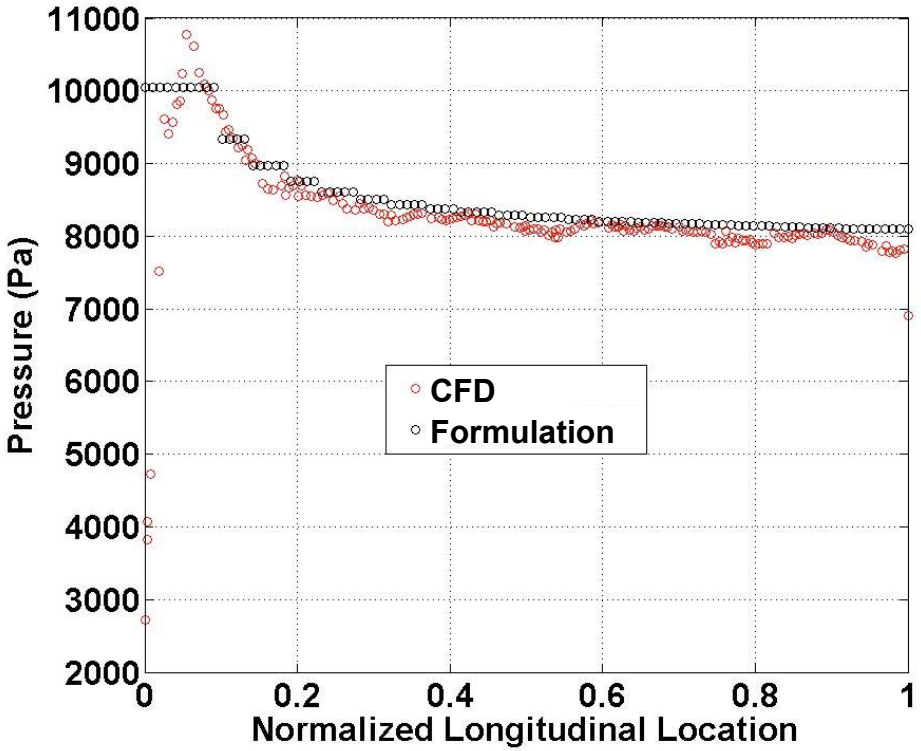

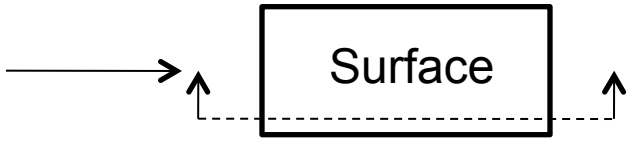

Close agreement with CFD data

Front Surface Pressure Contours
M=8, α=β=0

Formulation **CFD Results**

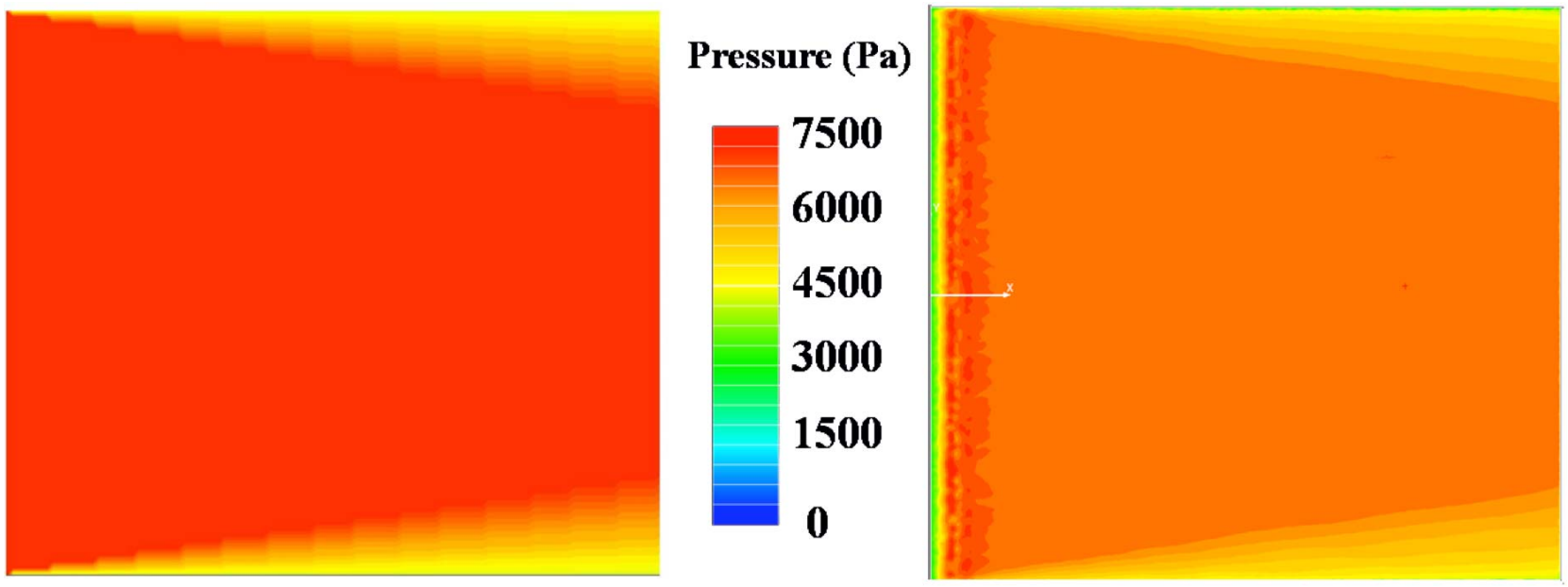

Qualitatively, pressure contours are similar

Downstream Surface

- Pass the 2-D shock values and Taylor-Maccoll boundary condition values through an expansion fan
- As before, linearly interpolate between boundary conditions and 2-D shock/expansion values
- Process repeated for any further downstream surface

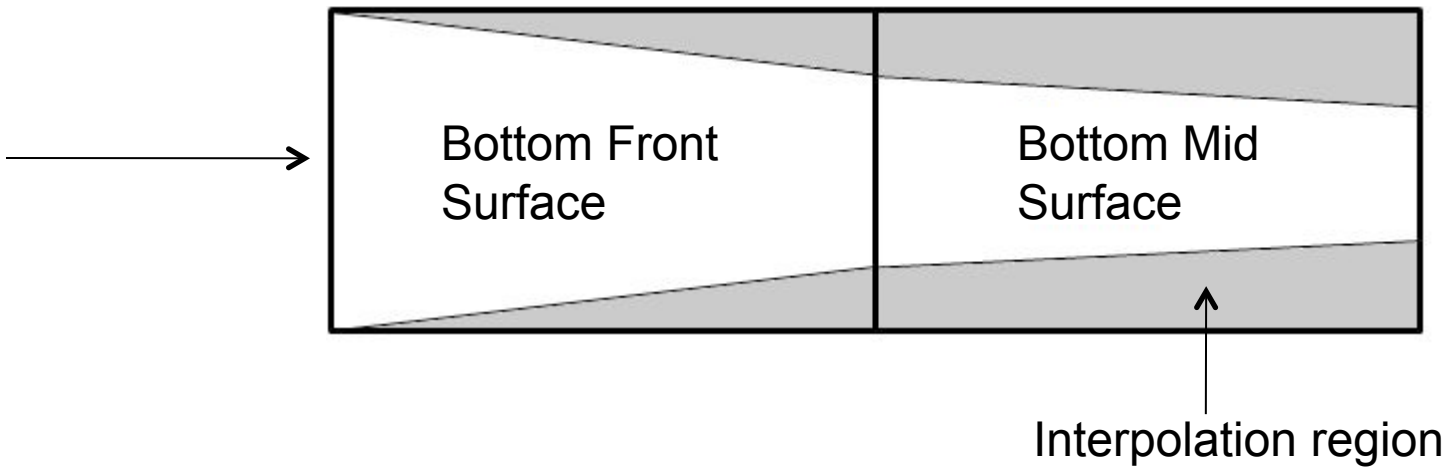

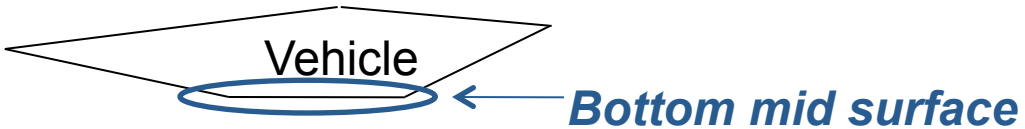

Bottom Mid Surface Pressure Comparisons

M=8, α=β=0

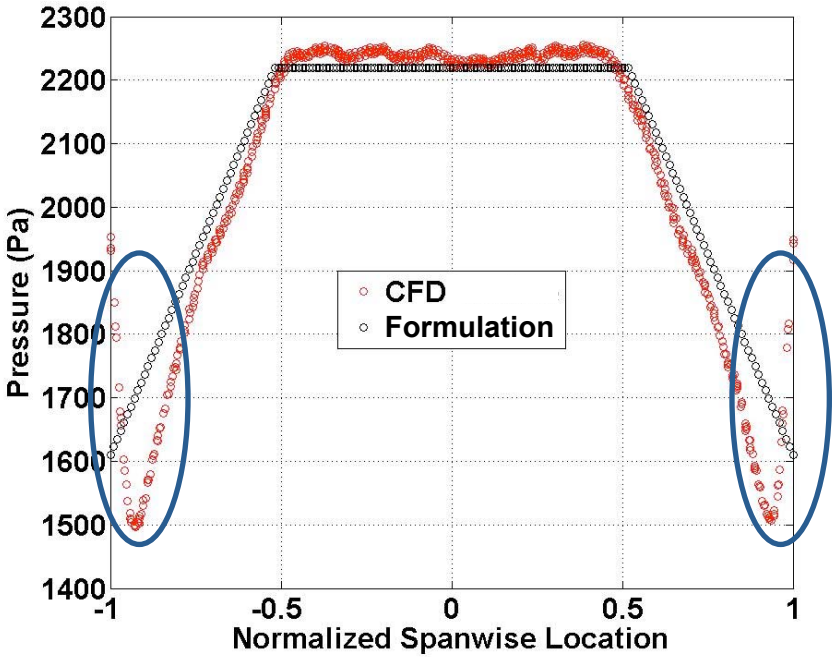

M=8, α=β=3˚

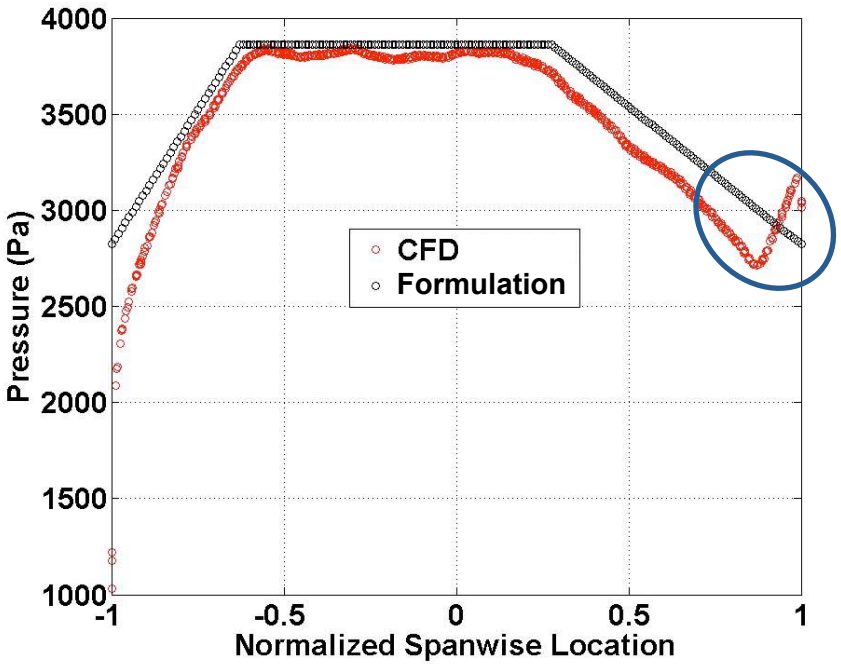

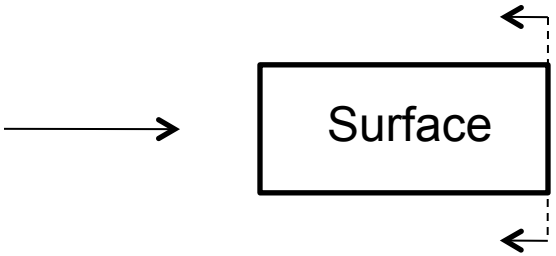

Good agreement, though some edge effects not captured by formulation

Mid Surface Pressure Contours
M=8, α=β=0

Formulation

CFD Results

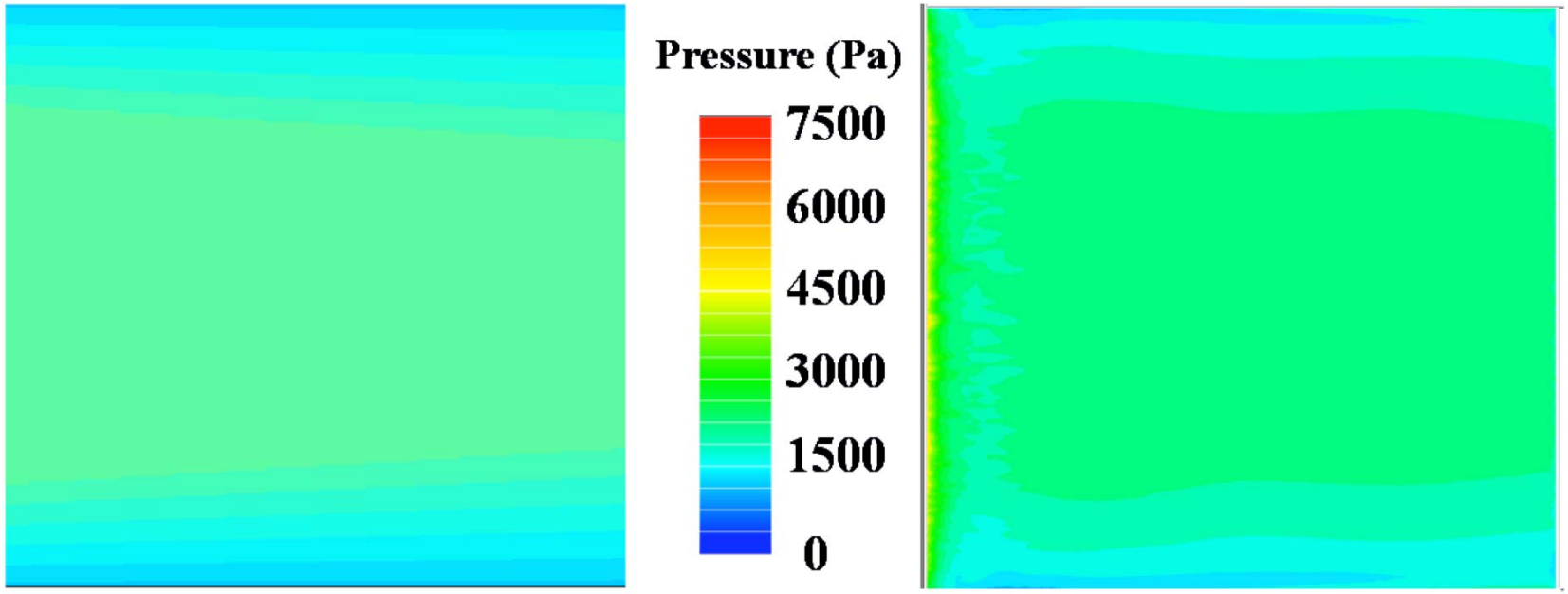

Qualitatively, pressure contours are similar

Force and Moment Calculations

- CFD runs conducted over range of α and β; examples shown on subsequent slide
- Resultant forces and moments on bottom front and bottom mid surfaces calculated
- Force and moment errors of formulation for each surface under 5% compared with CFD for all cases
- Increased accuracy over strictly two-dimensional pressures on each surface

- Note: on actual vehicle, engine would be on bottom mid surface; however, formulation simply looks at any situation where one surface is downstream of another

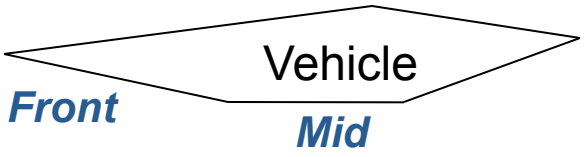

Example Force Calculations

Case			Percent Error: Front		Percent Error: Mid	
M	***α***	***β***	**Formulation**	**2-D**	**Formulation**	**2-D**
8	0	0	1.07	3.64	1.57	7.32
8	-3	0	0.28	2.24	-1.10	3.48
8	0	3	0.65	3.20	0.30	5.97
8	3	3	1.66	4.20	1.93	8.61
8	10	0	3.30	5.84	4.77	13.2
6	0	0	0.74	3.95	1.66	9.10
10	0	0	1.49	3.60	0.47	5.19
Average Improvement			**2.50**		**5.87**	

"2-D" uses pressure calculated from 2-D shock/expansion equations as pressure over entire surface

Errors increase as further downstream the surface is

Agenda

- Overall approach
- Top and bottom surface formulations
- ***Side surface formulation***
- Summary and future work

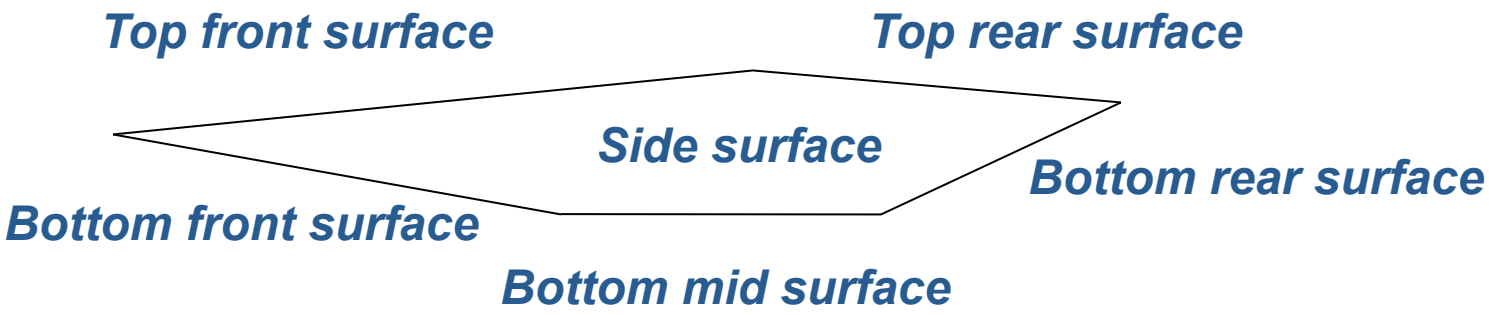

Side Formulation Overview

Top boundary pressure same as center pressure

Center pressure = combination of shock and conical flow or expansion pressures using angle of incidence ψ_s between side surface and freestream flow

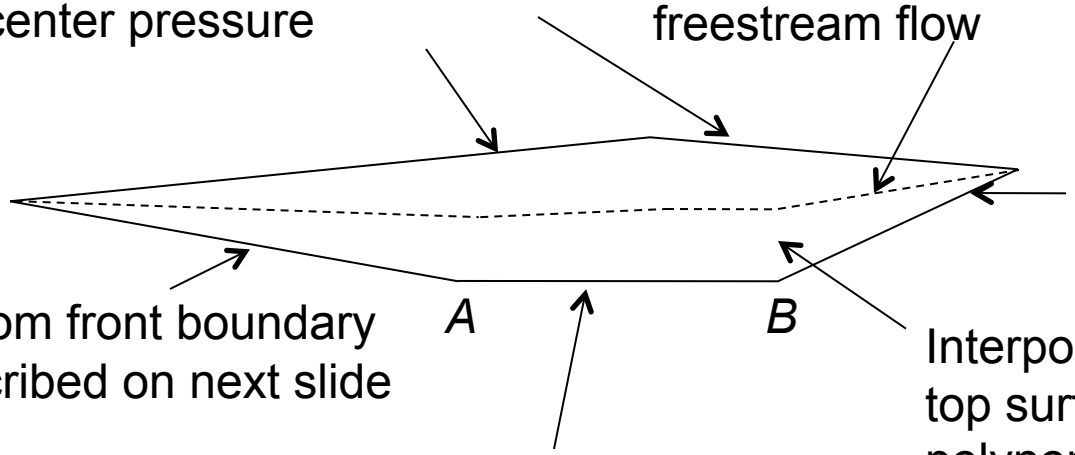

Bottom rear surface pressure = center pressure

Bottom front boundary described on next slide

Interpolation between bottom and top surfaces using 2nd order polynomial

Bottom mid surface pressures: linearly interpolate from A to B (based on observation of CFD pressure contours)

p_A=bottom front boundary pressure
p_B=center pressure

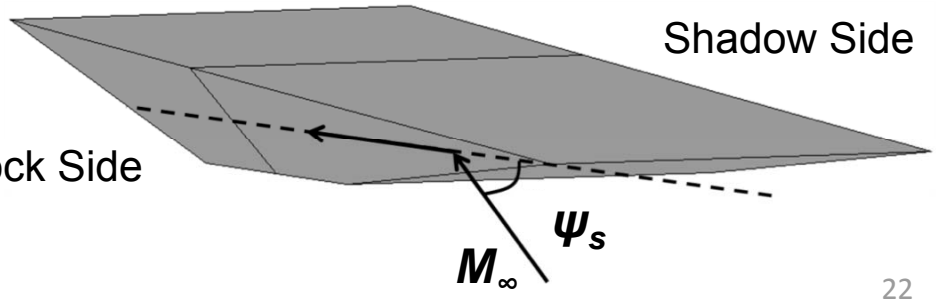

Side: Bottom Front Boundary Condition

- Bottom front surface has higher pressure in middle and lower pressure on edges, which will induce cross flow
- Flow velocity, etc. already known across surface; cross flow velocity vector added into known flow velocity vector on surface
- Expansion fan calculated for flow going over edge to side surface
- Quantities obtained used for side bottom boundary conditions
- If post-expansion pressure is greater than side midline pressure, interpolation not used; side pressure is constant midline pressure

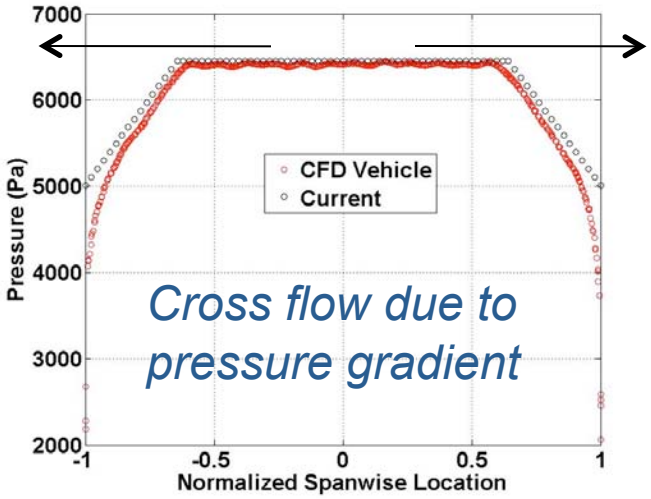

Bottom Front Surface Pressure Distribution

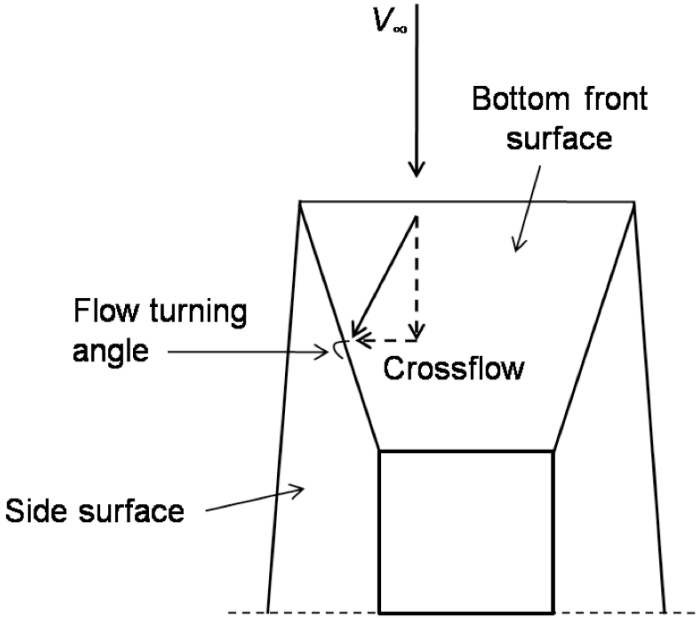

Side Surface Pressure Distributions

M=8, ψ_s=0˚, τ_{taper}=45˚

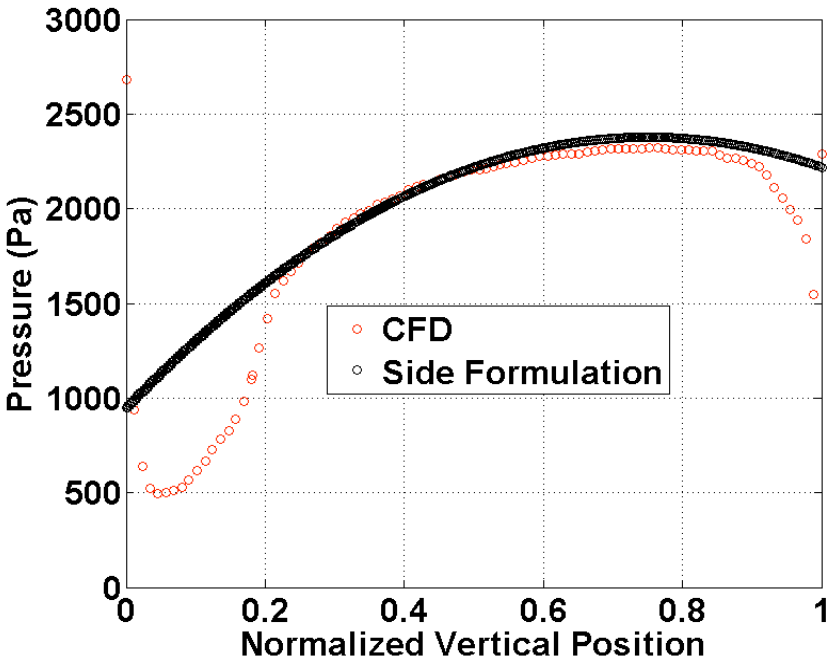

M=8, ψ_s=3˚, τ_{taper}=0˚

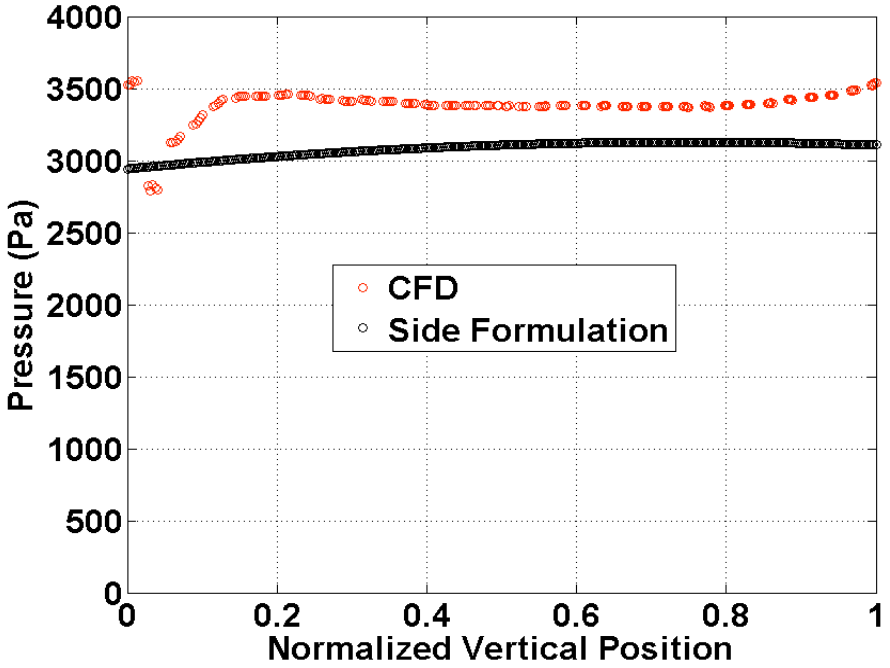

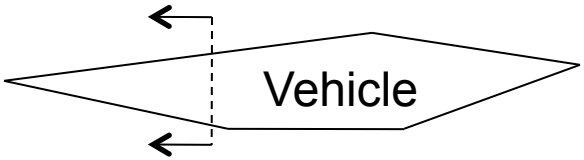

Side Surface Pressure Distributions

M=8, ψ_s=0˚, τ_{taper}=45˚

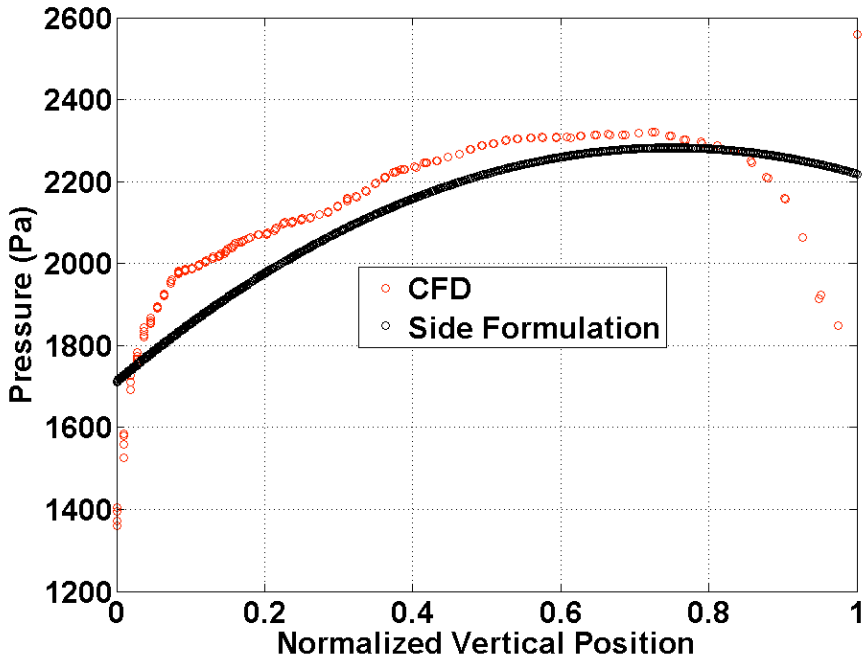

M=8, ψ_s=3˚, τ_{taper}=0˚

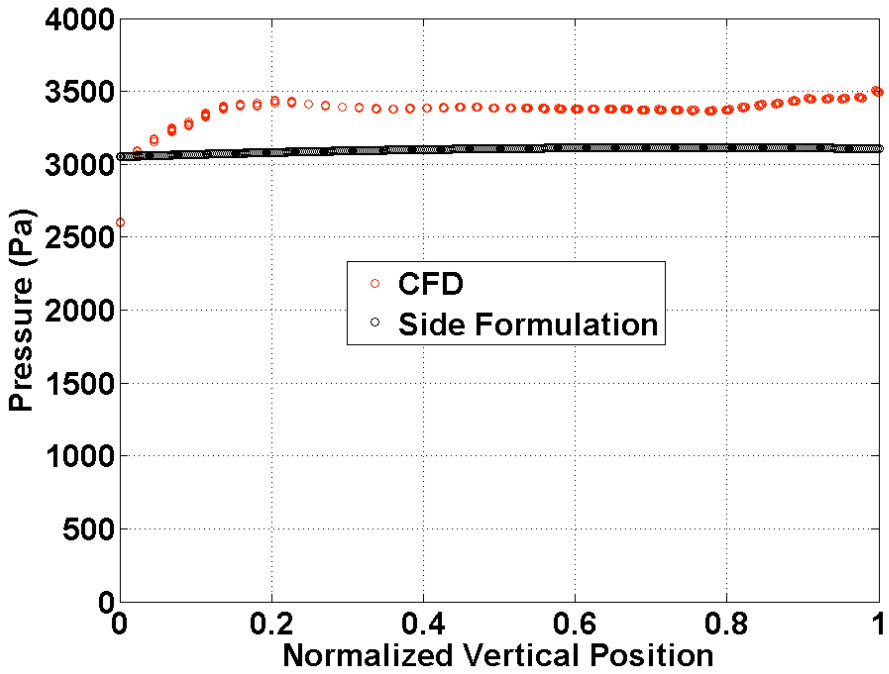

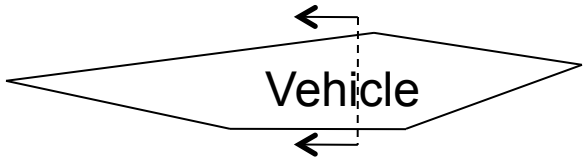

Side Formulation Results

- Compared with CFD, resultant force and moment errors remain small over range of ψ_s corresponding to shock side
  - ψ_s =0˚ (β=0°, τ_{taper} = 45°), percent error is ~1%
  - ψ_s =3˚ (β=3°, τ_{taper} = 0°), percent error ~8%
  - Errors in range tested generally under 10%
- Some shadow side errors are larger:
  - ψ_s =-3˚, percent error is ~15% (negative ψ_s → expansion)
  - Due to geometry, shadow side may have a weak shock instead of expansion; max error observed ~25%
  - Overall pressure values on shadow side are less than shock side, so larger percent errors will have less effect on vehicle dynamics

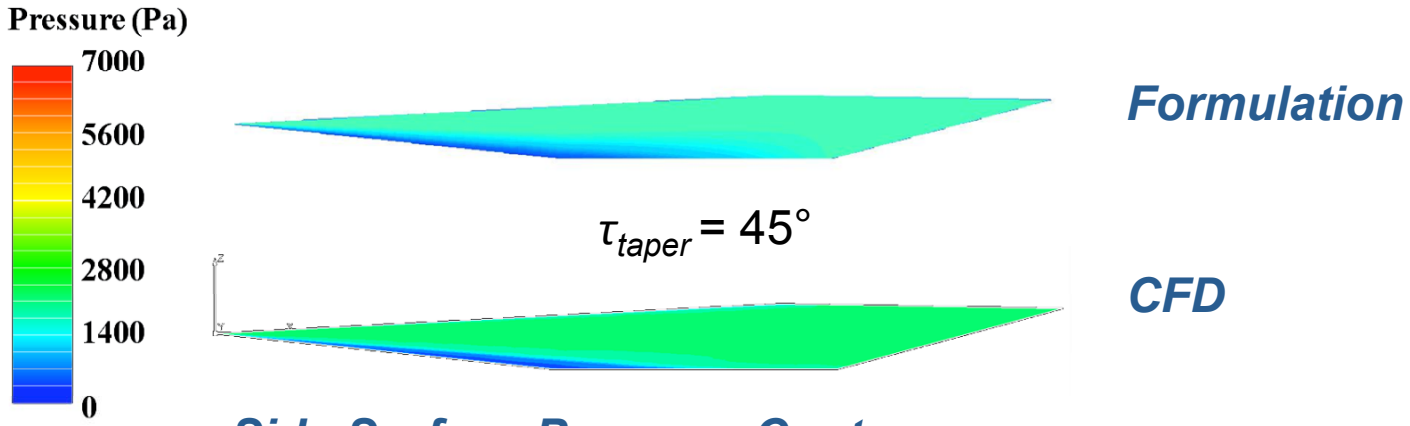

Side Surface Pressure Contours

Agenda

- Overall approach
- Top and bottom surface formulations
- Side surface formulation
- ***Summary and future work***

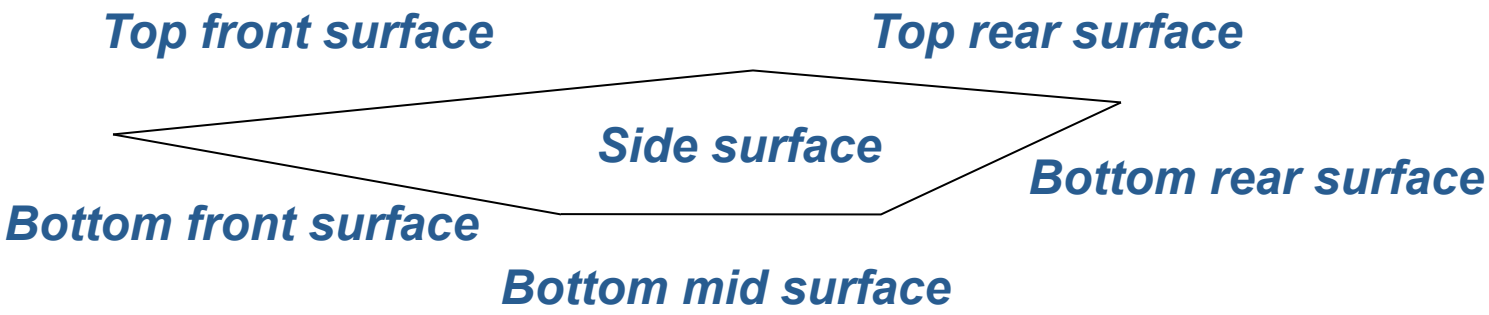

Summary and Future Work

- Goal: Create computationally efficient aeroelastic model of hypersonic vehicle
- Major milestones
  - Developed formulations for the pressure distributions over surfaces of 3-D hypersonic vehicle using combination of 2-D shock/expansion and conical flow equations
  - Compared formulations with Euler CFD solutions; good agreement in most cases
  - Implemented formulations into 6-DOF HSV simulation framework
- Future Work
  - Develop unsteady aerodynamic reduced-order model using Volterra series coupled with CFD simulations
  - Include viscous effects into steady aero model

Simulation Framework

Scott Frendreis
Carlos Cesnik

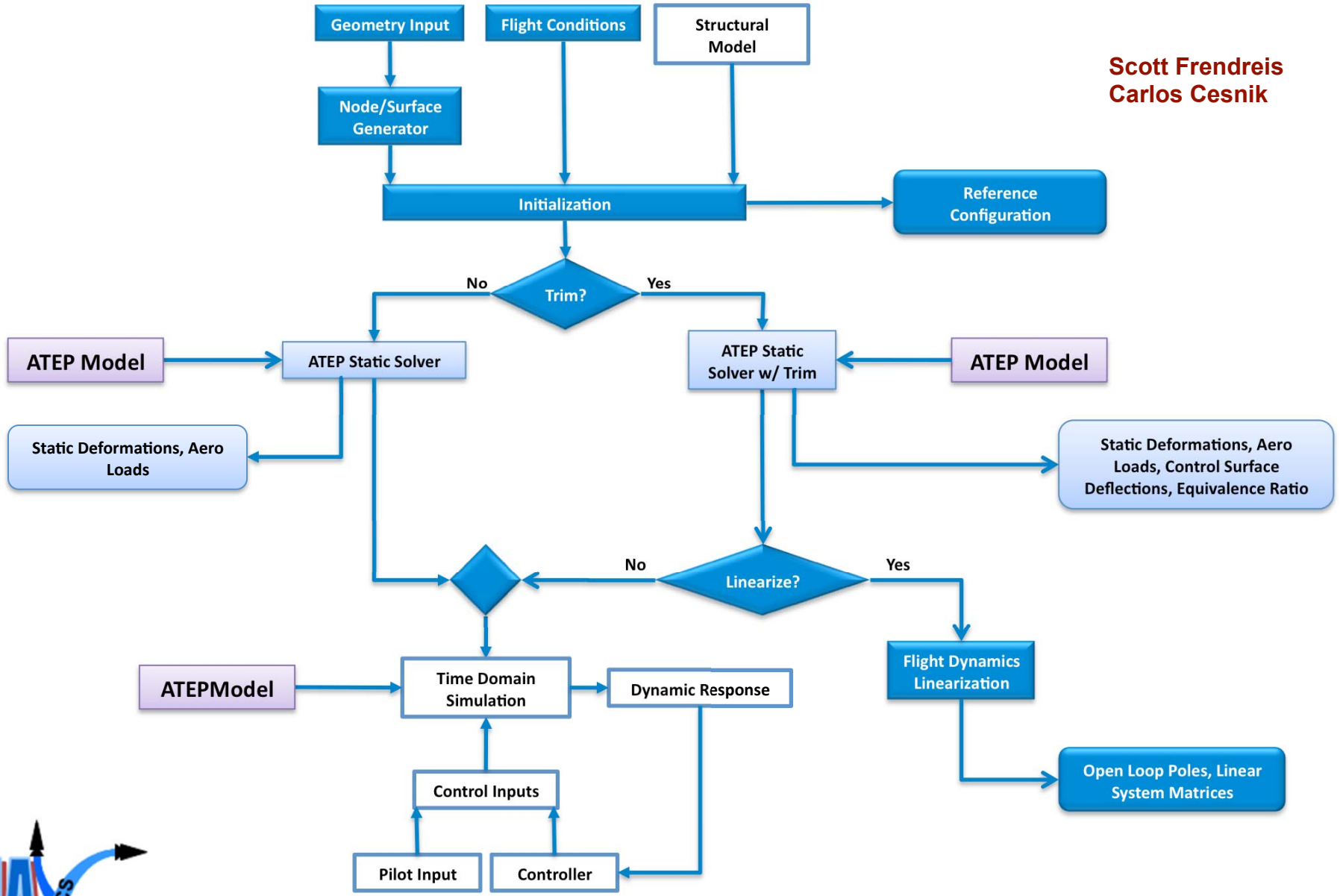

Relevant Publications

- **Published Papers**
  - Skujins, T., Cesnik, C.E.S., Oppenheimer, M.W., and Doman, D.,B. "Applicability of an Analytical Shock/Expansion Solution to the Elevon Control Effectiveness for a 2-D Hypersonic Vehicle Configuration," *Proceedings of the 2008 AIAA Atmospheric Flight Mechanics Conference and Exhibit*, August 2008
  - Oppenheimer, M.W., Skujins, T., Cesnik, C.E.S., and Doman, D.B., "Canard-Elevon Interactions on a Hypersonic Vehicle," *Proceedings of the 2008 AIAA Atmospheric Flight Mechanics Conference and Exhibit*, August 2008
  - Frendreis, S.G.V., Skujins, T., and Cesnik, C.E.S., "Six-Degree-of-Freedom Simulation of Hypersonic Vehicles," *Proceedings of the 2009 AIAA Atmospheric Flight Mechanics Conference*, August 2009
- **Planned Papers**
  - Skujins, T., Cesnik, C.E.S., Oppenheimer, M.W., and Doman, D.B., "Canard-Elevon Interactions on a Hypersonic Vehicle," Journal of Spacecraft and Rockets, accepted
  - 2010 AFM Conference

Reduced-Order Thermoelastic Modeling of Hypersonic Vehicles

Nate Falkiewicz

Carlos E. S. Cesnik

Aerospace Engineering Department

University of Michigan, Ann Arbor

Michigan AFRL Collaborative Center in Control Sciences

Ann Arbor, MI, September 23-24 2009

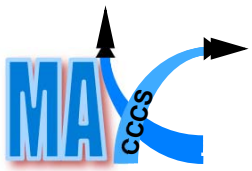

Task Summary

- **Nate Falkiewicz (AFRL, Cesnik)** – Thermo-structural modeling of HSV and its control surfaces
  - Develop techniques for extracting reduced order thermal and structural models
    - Developed Proper Orthogonal Decomposition (POD) formulation for reduced order transient thermal analysis
    - Implemented modified modal formulation for reduced order (modal) structural dynamic representation
  - Assess heat flow and its impact on elastodynamic characteristics of HSV and its control surfaces
    - Performed initial assessment of effect of material degradation and thermal stresses on natural frequencies and structural response
    - Created finite element representation of HSV control surface for aerothermoelastic analysis
  - Create variable-fidelity models for thermo-structural control design and control evaluation representations

Agenda

- Motivation and Problem Overview
- Reduced Order Thermal Modeling
- Reduced Order Structural Dynamic Modeling
- Study of Effect of Structural Deformation on Aerodynamic Forces
- Summary and Future Work

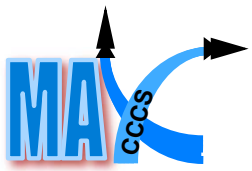

Motivation

- Control simulation and vehicle design requires low order models that are computationally efficient and possess a low number of states
- Due to high speed, time varying heat flux exists at vehicle surface
- Results in heat being conducted through internal structure → *need to know detailed heat path to determine local temperatures*
- Temperature-dependent Modulus and thermal stress modifies stiffness
  - Change in stiffness affects structural frequencies and mode shapes
  - Alters vehicle dynamics/controllability and control surface effectiveness

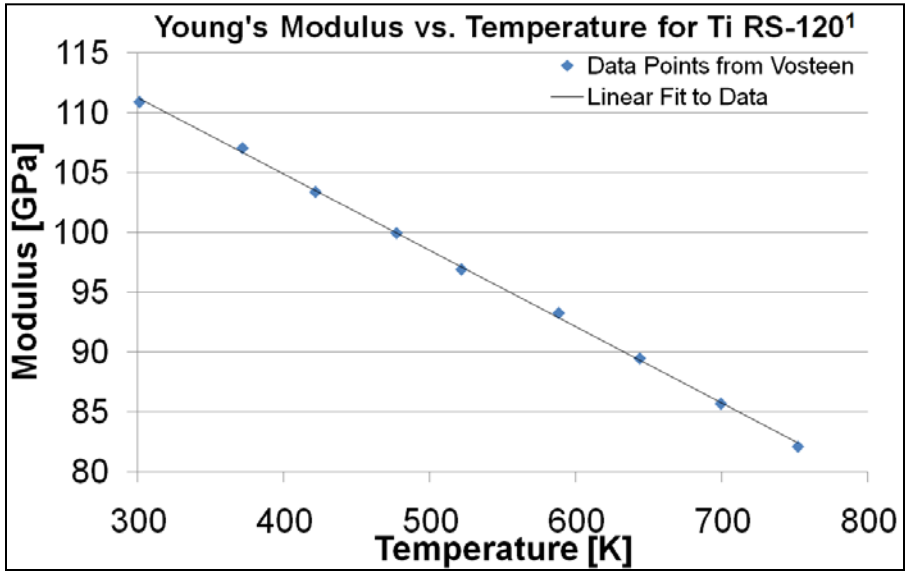

Modulus decreases with increasing temperature

$$[m]\{\ddot{q}\}+[k(T)]\{q\}=\{f(t)\}$$

Equations of motion now a function of temperature

[1]Vosteen, L.F., "Effect of Temperature on Dynamic Modulus of Elasticity of Some Structural Alloys, NACA TN 4348, Langley Aeronautical Laboratory, Langley Field, VA, Aug. 1958

Thermoelastic Reduced Order Modeling Framework

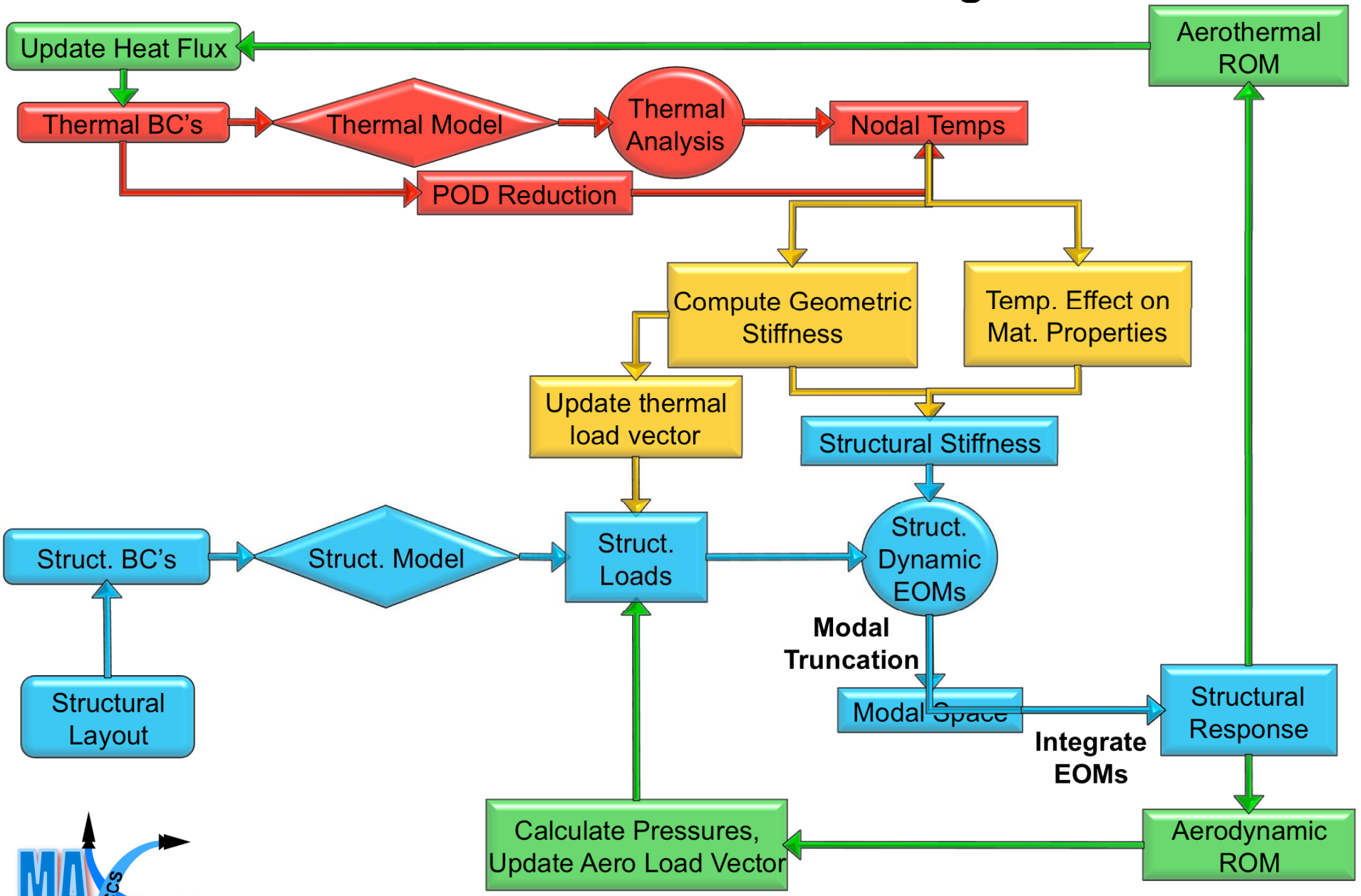

High-fidelity solution infeasible, must use reduced-order methods

HSV Control Surface Model Example

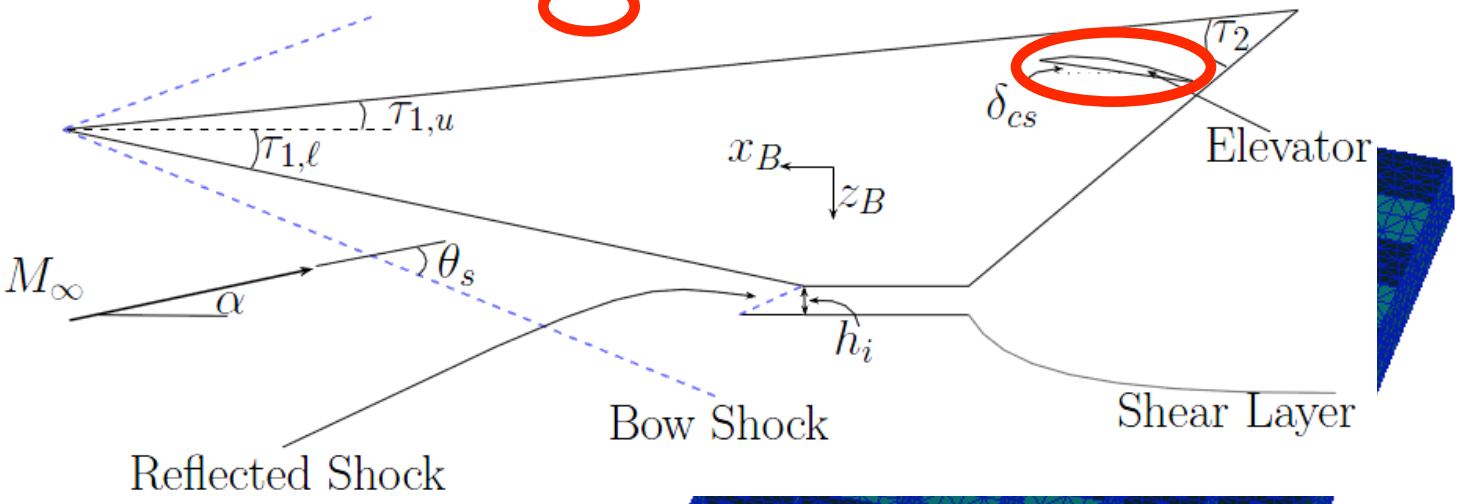

2D HSV schematic from Bolender, Doman, 2005 (AIAA-2005-6255)

Control Surface Finite Element Model With Top Skin Hidden (9,200 elements)

3D HSV Configuration from Frendreis, Skujins, Cesnik, 2009 (AIAA-2009-5601)

Agenda

- Motivation and Problem Overview
- Reduced Order Thermal Modeling
- Reduced Order Structural Dynamic Modeling
- Effect of Structural Deformation on Aerodynamic Forces
- Summary and Future Work

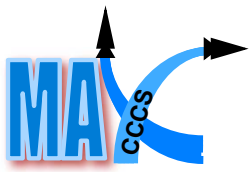

Use of POD Modes for Thermal Solution

- Want to express vector of nodal temperatures as:

$$\begin{Bmatrix} T_1 \\ \vdots \\ T_m \end{Bmatrix} = c_1(t)\begin{Bmatrix} \varphi_1^{(1)} \\ \vdots \\ \varphi_m^{(1)} \end{Bmatrix} + c_2(t)\begin{Bmatrix} \varphi_1^{(2)} \\ \vdots \\ \varphi_m^{(2)} \end{Bmatrix} + \ldots + c_n(t)\begin{Bmatrix} \varphi_1^{(n)} \\ \vdots \\ \varphi_m^{(n)} \end{Bmatrix}$$

POD Basis vectors, derived from high-fidelity snapshots

- The above can be expressed in matrix form if we assemble the modal matrix, Φ, whose columns are the basis vectors from the above expansion

$$\begin{Bmatrix} T_1 \\ \vdots \\ T_m \end{Bmatrix} = \underbrace{\begin{bmatrix} \varphi_1^{(1)} & \varphi_1^{(2)} & \cdots & \varphi_1^{(n)} \\ \varphi_2^{(1)} & \varphi_2^{(2)} & \cdots & \varphi_2^{(n)} \\ \vdots & \vdots & \cdots & \vdots \\ \varphi_m^{(1)} & \varphi_m^{(2)} & \cdots & \varphi_m^{(n)} \end{bmatrix}}_{\Phi\ (m \times n)} \underbrace{\begin{Bmatrix} c_1(t) \\ \vdots \\ c_n(t) \end{Bmatrix}}_{n \times 1} = [\Phi]\{c\}$$

Number of DOFs is reduced from m to n, n << m

- Basis will be truncated, so $n << m$ and the number of DOFs is reduced

Determination of POD Basis Vectors

- POD comes in when finding reduced basis vectors, $\{\varphi^{(i)}\}$
- Find N_s mode shapes ("snapshots"). In this case, snapshots are vectors of nodal temperatures at different time steps from high-fidelity transient thermal FEA
- Assemble snapshot matrix, A:

$$[A]=\begin{bmatrix} T_1^{(1)} & T_1^{(2)} & \cdots & T_1^{(N_s)} \\ T_2^{(1)} & T_2^{(2)} & \cdots & T_2^{(N_s)} \\ \vdots & \vdots & \cdots & \vdots \\ T_m^{(1)} & T_m^{(2)} & \cdots & T_m^{(N_s)} \end{bmatrix}$$

- Find correlation matrix taking advantage of finite element shape functions:

$$C_{ij}=\frac{1}{N_s}\int_V \{T^{(i)}\}^T \{T^{(j)}\} dV = \frac{1}{N_s}\sum_e \left[\{T_e^{(i)}\}^T \int_V \left([N]^T [N] dV \right) \{T_e^{(j)}\} \right]$$

- Eigenvalues, λ, and eigenvectors, v, of correlation matrix used to form POD basis, φ, from snapshots

$$\varphi_k = \frac{1}{\sqrt{N_s \lambda_k}} \sum_{i=1}^{N} v_i^{(k)} A^{(i)}$$

Optimality of POD Basis

- Eigenvalues of correlation matrix related to significance of each POD mode
- Inherent correlation of snapshots leads to rapid decay of eigenvalues
- POD modes whose corresponding eigenvalues are small can be eliminated, thus allowing for reduction in DOFs

Semi-log plot of eigenvalues vs. mode number

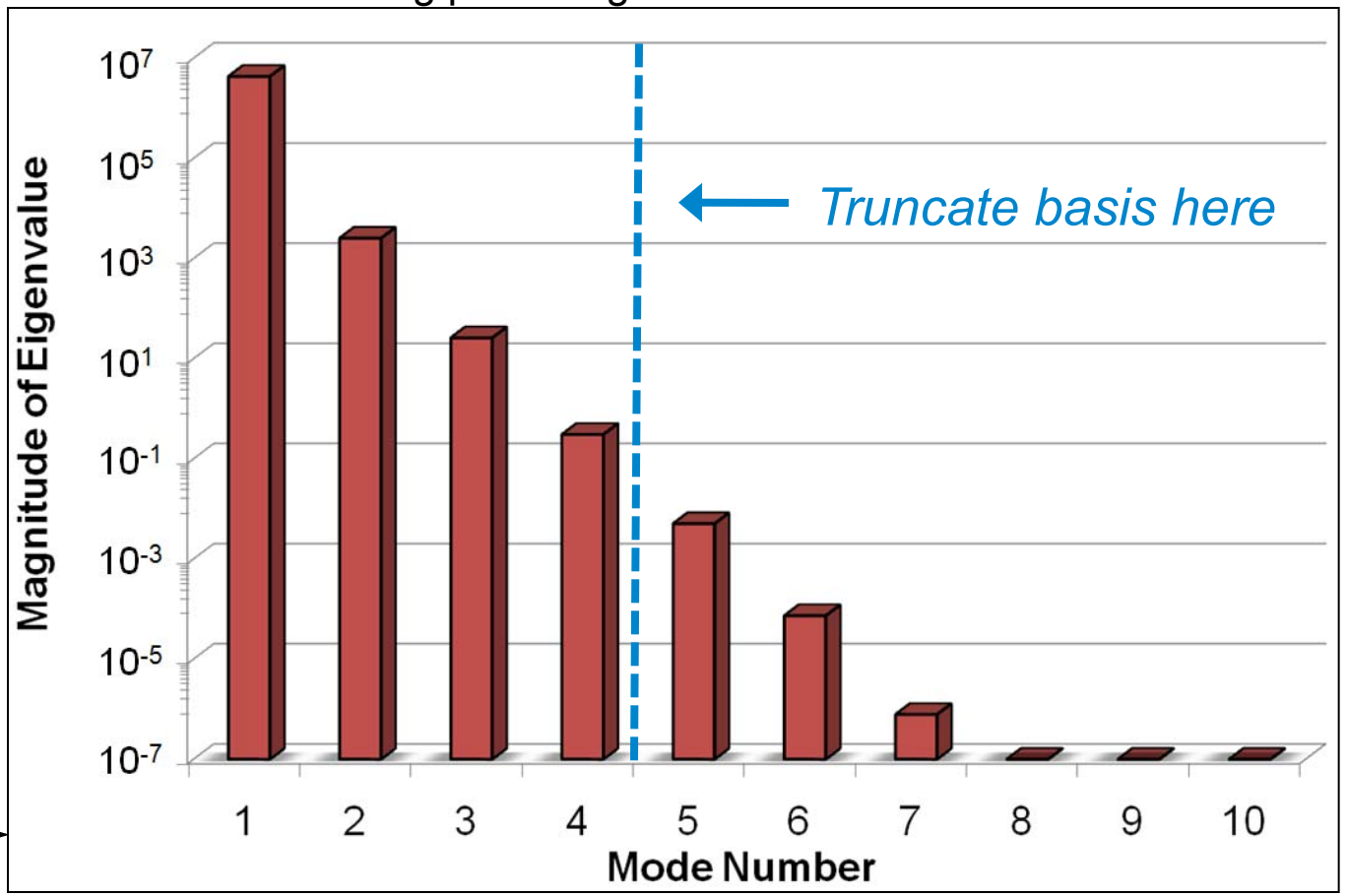

FEM contains 4,056 DOFs, only 4 DOFs included in ROM

Equation Transformations in Thermal Solution[1]

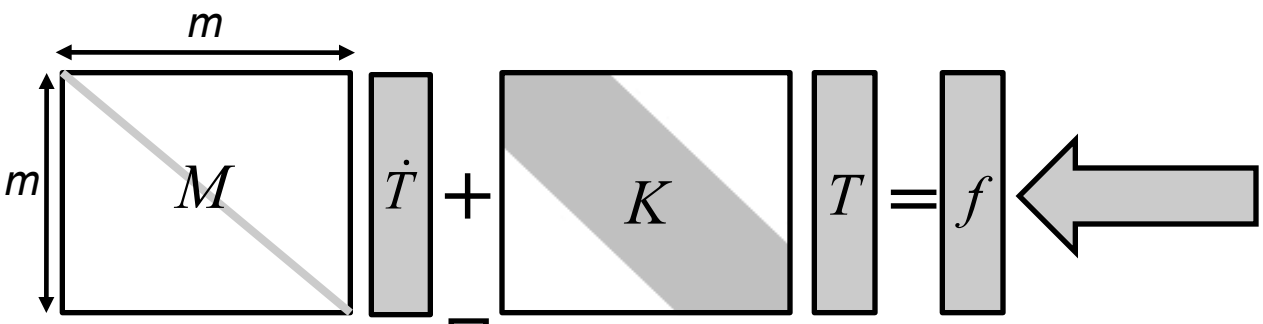

Original system of equations

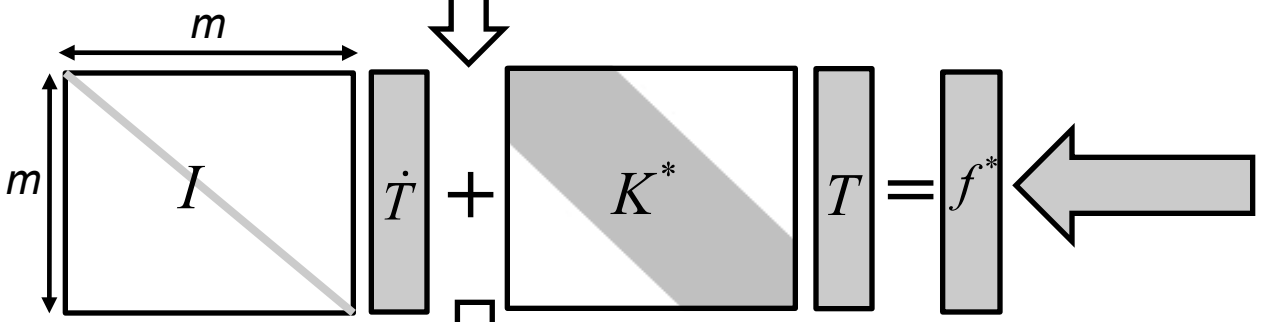

Capacitance matrix normalized to unit magnitude

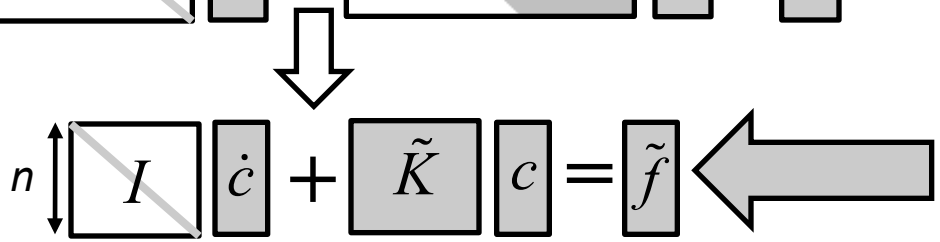

Transformed to modal space using POD modes, problem is reduced

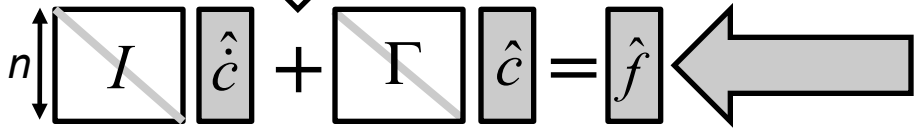

Coefficient matrix diagonalized to decouple equations

[1]Bialecki, R., Kassab, A., and Fic, A., "Proper orthogonal decomposition and modal analysis for acceleration of transient FEM thermal analysis," *Int. J. Numer. Eng.* 2005; 62:774-797

Control Surface Case with Constant Heat Flux

- Applied POD to control surface finite element model (4,056 DOFs)
- Used 26 snapshots at 20 s intervals from 0 – 500 s, included 4 POD modes
- Applied constant, uniform heat flux of 10 W/cm^2 to top skin only. Initial condition is uniform room temp
- Note:
  - Plan to update control surface model to include aerodynamic profile for use in aeroheating calculations
  - Future work will incorporate aeroheating analysis being conducted at OSU to give accurate spatial representation of heat flux boundary condition

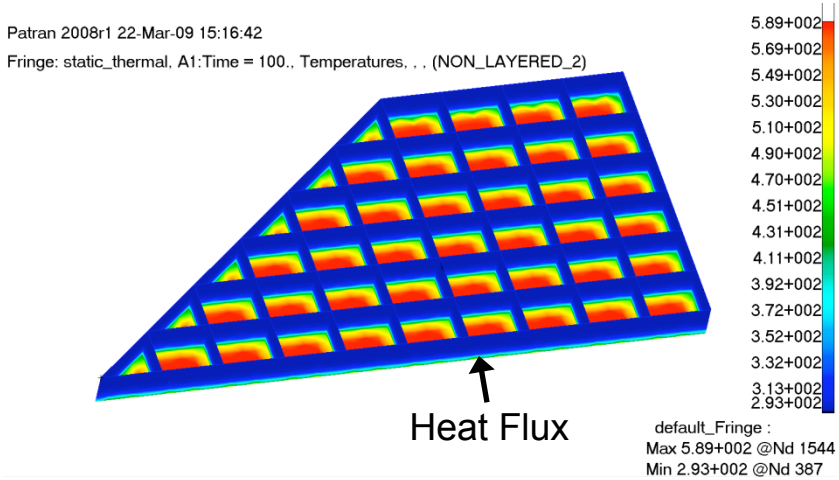

Temperatures [K] at t = 100 s

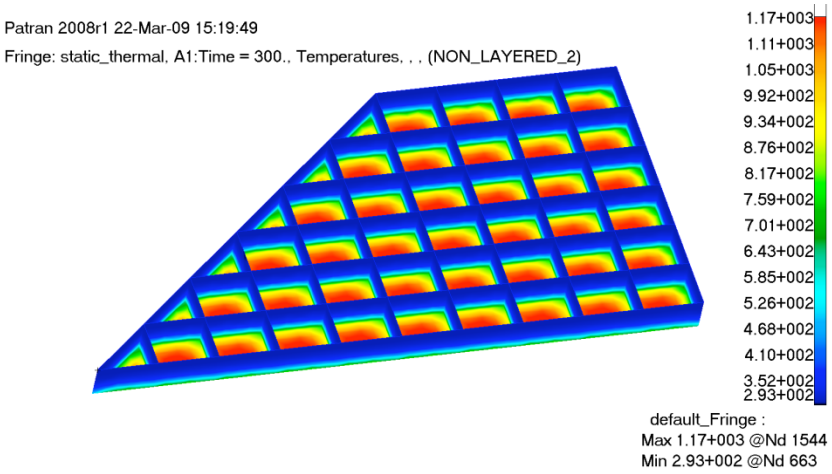

Temperatures [K] at t = 300 s

POD vs. Thermal FEA Results for Constant Heat Flux

- Ran POD code and calculate temperature distribution at various time steps
- Compared nodal temperatures from POD with those from Nastran
- Error vector defined as: $\{\text{Error}\} = \text{abs}\left(\{T_{FEA}\} - \{T_{POD}\}\right)$
- Percent error at node *i* defined as: $(\%\ \text{Error})_i = \dfrac{\text{abs}\left[(T_{FEA})_i - (T_{POD})_i\right]}{(T_{FEA})_i} \times 100$

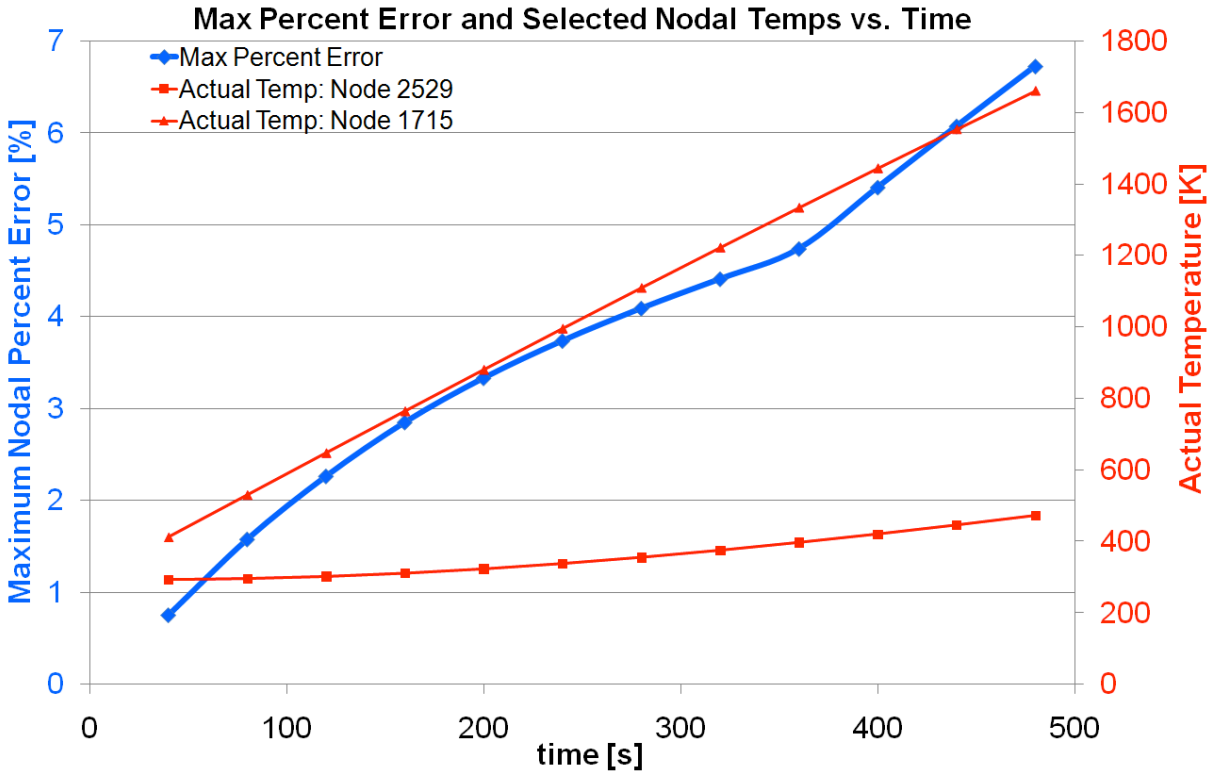

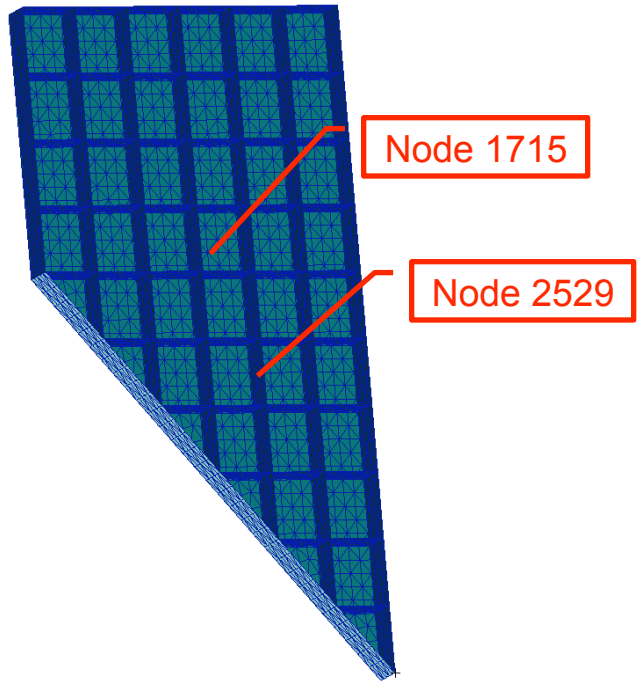

Plan to investigate effect of number of snapshots and basis vectors

POD with Time-Dependent Heat Flux

- Modes are admissible functions and only need to satisfy geometric boundary conditions (fixed temperature BC's)
- Model only contains natural boundary conditions (heat flux BC's)
- Conclusion: POD modes do not need to be updated as heat flux changes. FEA only needed for initial offline generation of basis vectors

Performing modal expansion on the RHS:

$$\{\dot{\hat{c}}\} + \begin{bmatrix} \diagdown & & \\ & \Gamma & \\ & & \diagdown \end{bmatrix} \{\hat{c}\} = \{\hat{f}(t)\}$$

Analytical solution to the above is:

$$\hat{c}(t) = \exp\left[-\gamma_i t\right] \int_0^t \mathrm{e}^{(\gamma_i t')} \hat{f}(t')\, dt'$$

- ***Heat flux depends on deformation → not known ahead of time***
- ***ROM methodology can handle time-dependent thermal BC's without need to return to high-fidelity model***

Agenda

- Motivation and Problem Overview
- Reduced Order Thermal Modeling
- Reduced Order Structural Dynamic Modeling
- Effect of Structural Deformation on Aerodynamic Forces
- Summary and Future Work

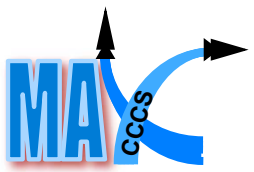

Modified Modal Representation of Structural Dynamics

- Stiffness matrix will be modified due to material degradation and thermal stress

$$[m]\{\ddot{q}\}+\left([k(T)]+\left[k_g(T)\right]\right)\{q\}=\{f(t)\},\ \text{where}\ \left[k(T)\right]+\left[k_g(T)\right]\equiv\left[k^*(T)\right]$$

Conventional stiffness matrix

Geometric stiffness matrix due to thermal stresses

- If stiffness were constant, free vibration modes would diagonalize equations of motion

$$[\Phi]^T[m][\Phi]\{\ddot{\eta}\}+[\Phi]^T[k][\Phi]\{\eta\}=[\Phi]^T\{f(t)\}\Rightarrow\begin{bmatrix}\ddots & \\ & M_{rr} \\ & & \ddots\end{bmatrix}\{\ddot{\eta}\}+\begin{bmatrix}\ddots & \\ & \omega_r^2 M_{rr} \\ & & \ddots\end{bmatrix}\{\eta\}=\begin{Bmatrix}\\ F(t)\\ \\ \end{Bmatrix}$$

- Modes will change at every time step due to heating. Use free vibration modes at some reference temperature case since they are admissible functions

$$\left[\Phi_{ref}\right]^T[m]\left[\Phi_{ref}\right]\{\ddot{\eta}\}+\left[\Phi_{ref}\right]^T\left[k^*(T)\right]\left[\Phi_{ref}\right]\{\eta\}=\left[\Phi_{ref}\right]^T\{f(t)\}$$

- Stiffness matrix no longer diagonalized by reference modes since it is changing at every time step.

Equations of motion will now be coupled

Transformations in Structural Dynamics Equations

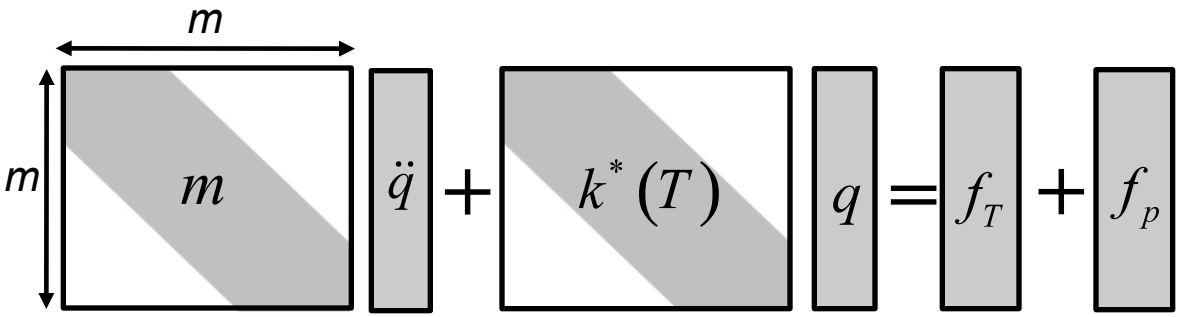

Original system of equations

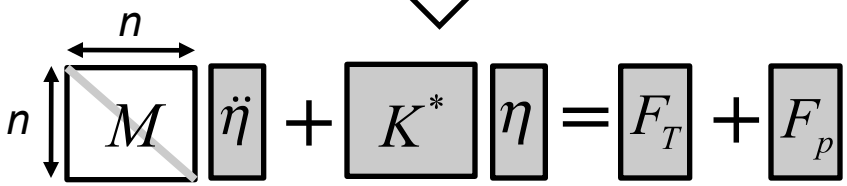

Equations transformed to modal space using $[\Phi_{ref}]$, problem is reduced

$$\{\eta_{n+1}\} = \{\eta_n\} + \{\dot{\eta}_n\}h + \left[(1-2\beta)\{\ddot{\eta}_n\} + 2\beta\{\ddot{\eta}_{n+1}\}\right]\frac{h^2}{2}$$

Equations of motion integrated to find modal coordinates

$$\{q_{n+1}\} = \left[\Phi_{ref}\right]\{\eta_{n+1}\}$$

Displacements transformed back to physical space

Initial Assessment of Impact of Thermal Stress

- Applied uniform heat flux of 10 W/cm^2 to bottom surface of finite element model
- Temperature distributions generated from POD
- Nastran Statsub card used to generate geometric stiffness
  - Adds static subcase prior to normal modes solution to solve static problem and generate geometric stiffness
  - Used Nastran DMAP alter to write geometric stiffness to output file
- Used temperatures at 320 seconds into thermal transient as sample case
- Note: *Plan to update heat flux with representative values and include radiation effects*

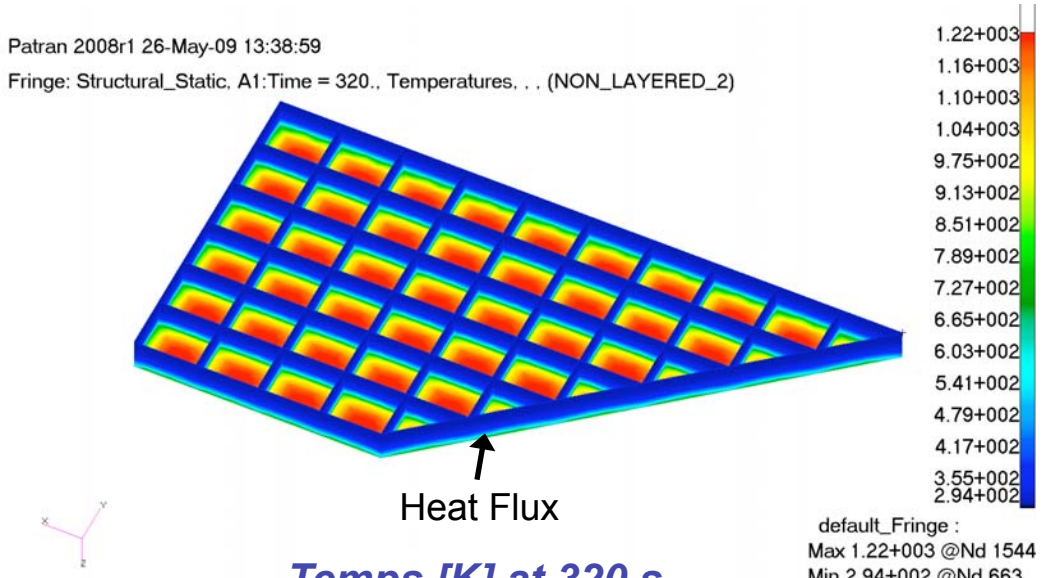

Temps [K] at 320 s

Differential thermal expansion results in spatially varying stress distribution

Initial Natural Frequency Results

- Calculated frequencies with material degradation (Young's Modulus decreasing with temperature) and thermal stress effects
- Initial results show thermal stress
  - has no significant effect on nominal lower natural frequencies
  - adds low frequency modes that otherwise would only show up at higher frequencies
- Effect is dependent on mode number

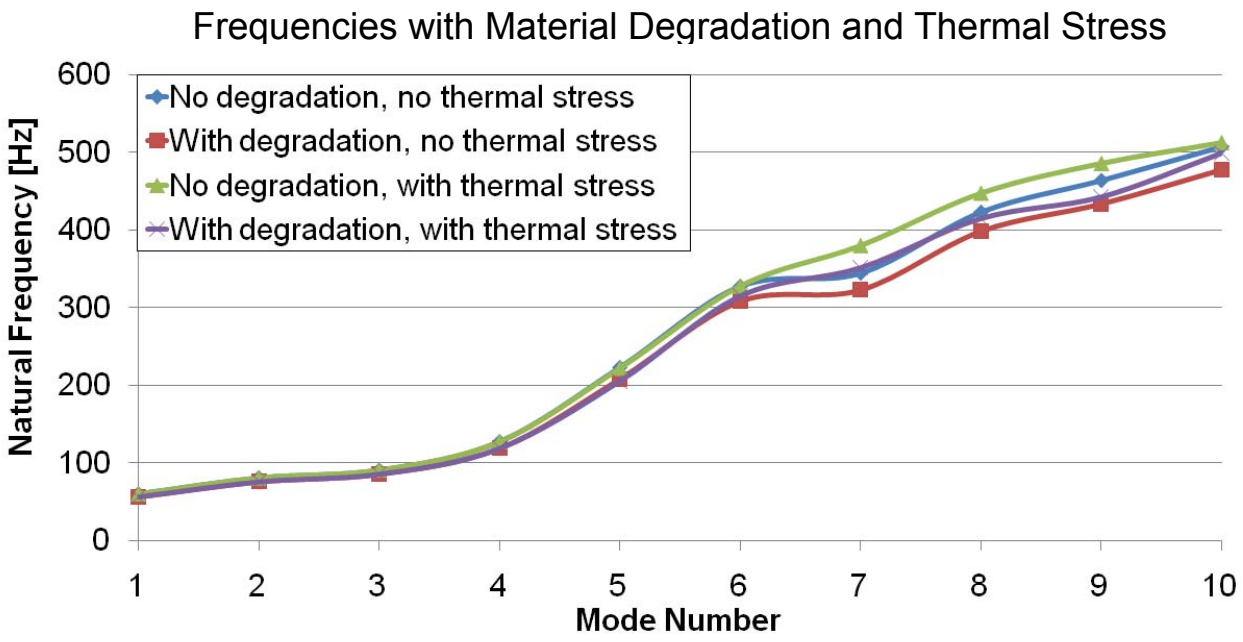

Mode shapes with material degradation and thermal stress

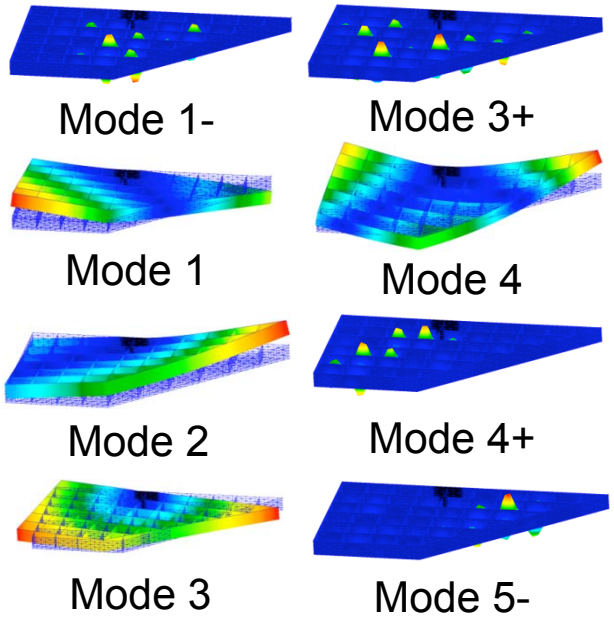

Example will be repeated on an updated structural model based on allowable temperatures, displacements, and stresses

Agenda

- Motivation and Problem Overview
- Reduced Order Thermal Modeling
- Reduced Order Structural Dynamic Modeling
- Effect of Structural Deformation on Aerodynamic Forces
- Summary and Future Work

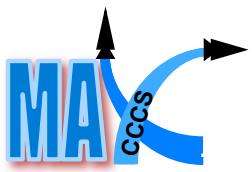

Aerothermoelastic Simulation Framework

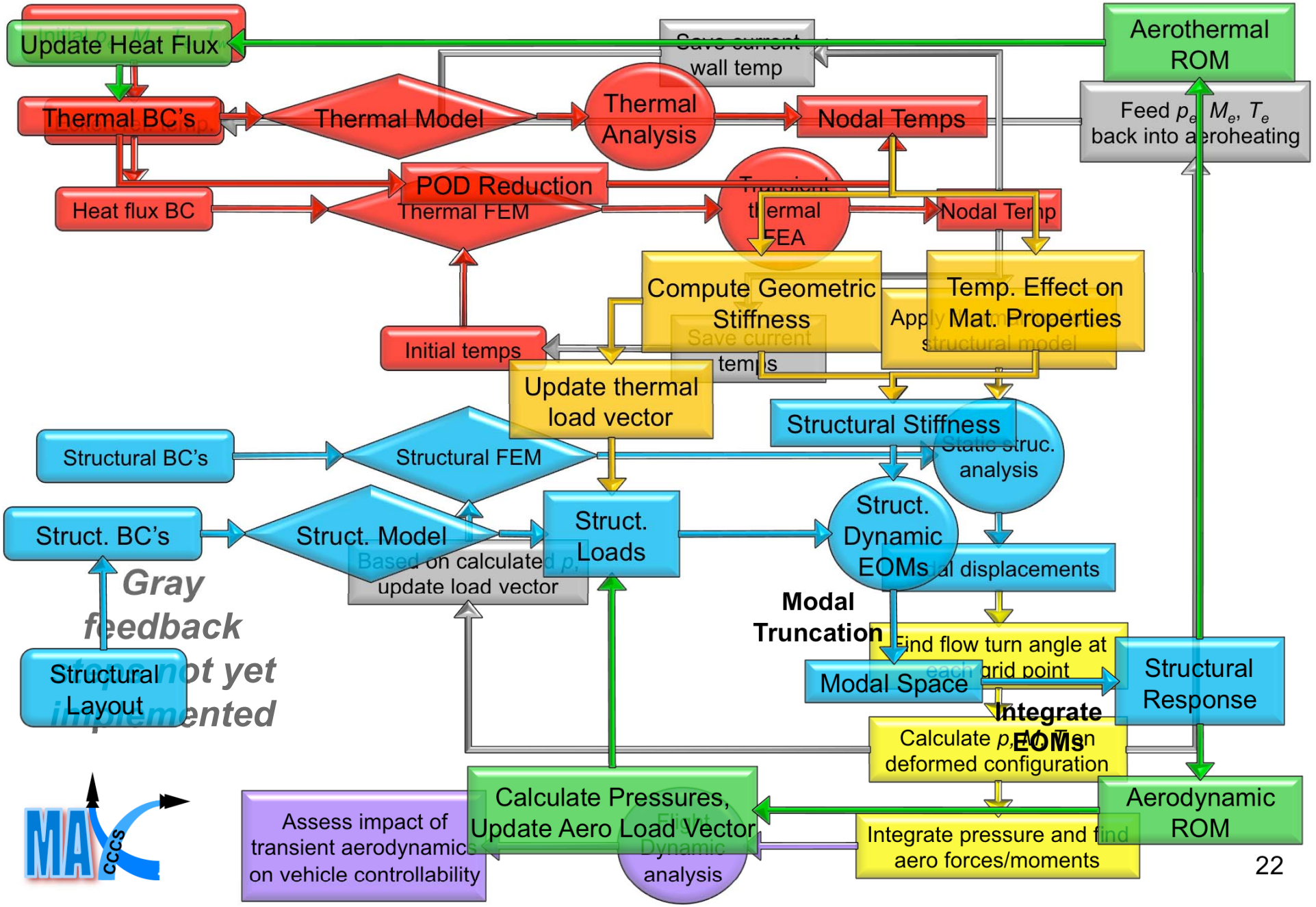

Aerothermal Modeling

- Heat flux calculated using undeformed configuration with flow properties from shock/expansion relations. Not yet updated as structure deforms

Freestream Flow

$M = 8$

$p = p_\infty$

$T = T_\infty$

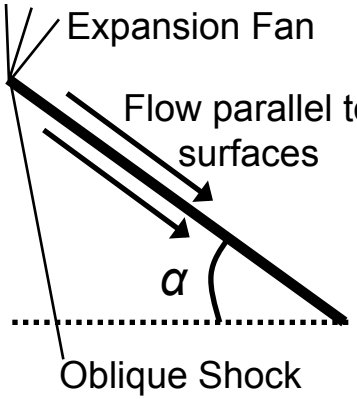

Schematic of flow over undeformed control surface

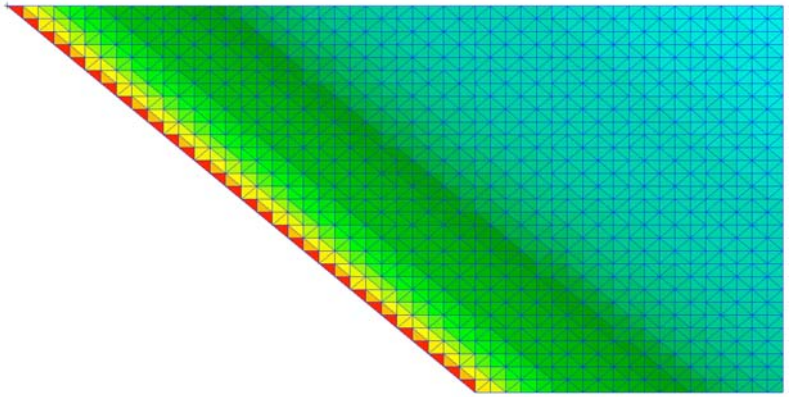

Heat flux [W/m²] on bottom surface

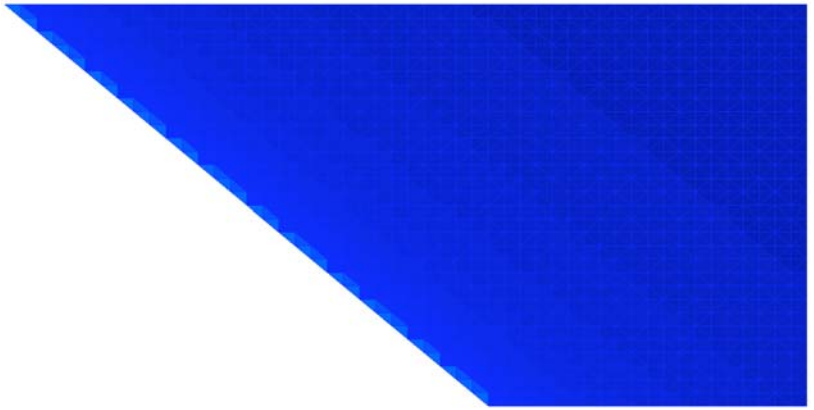

Heat flux [W/m²] on top surface

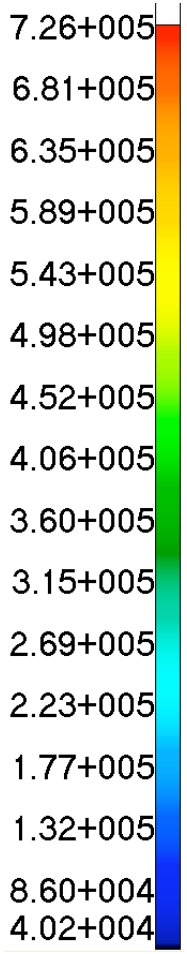

Heat flux higher on bottom surface due to angle of attack, decreases along chord due to Re dependence

Transient Thermal Finite Element Solution

- Transient temperature distribution calculated at discrete time intervals using Nastran
- Heat flux not yet updated as structure deforms

Top Isometric View (Skins Hidden) | **Top Isometric View** | **Bottom Isometric View**

Temperature Distribution [K] at 50 s

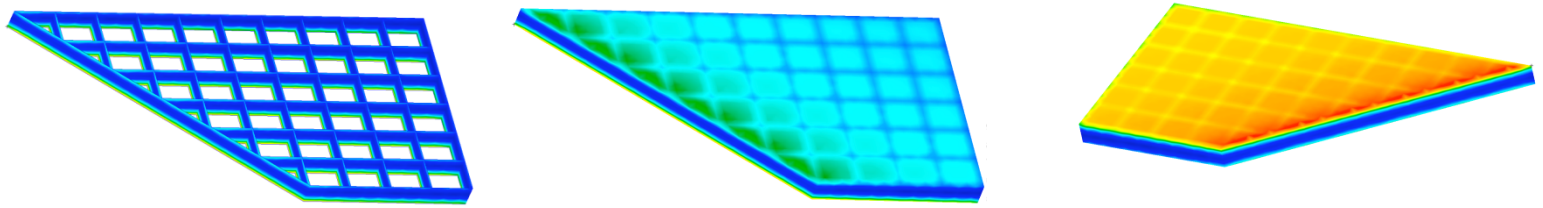

Temperature Distribution [K] at 300 s

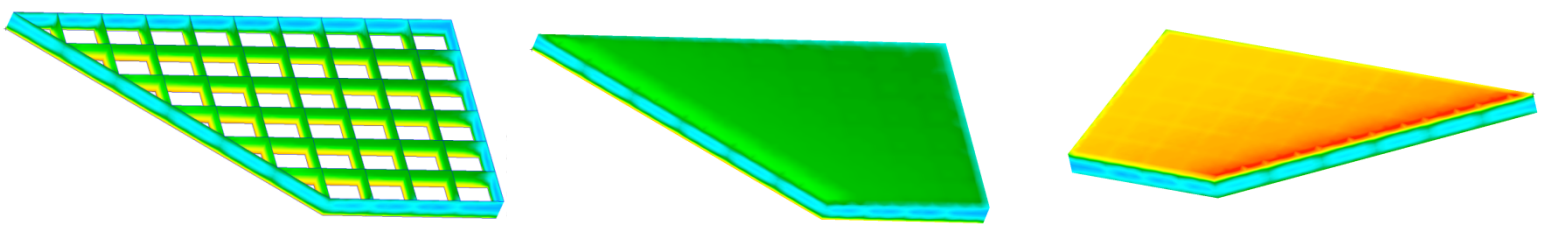

Temperature Distribution [K] at 2,000 s

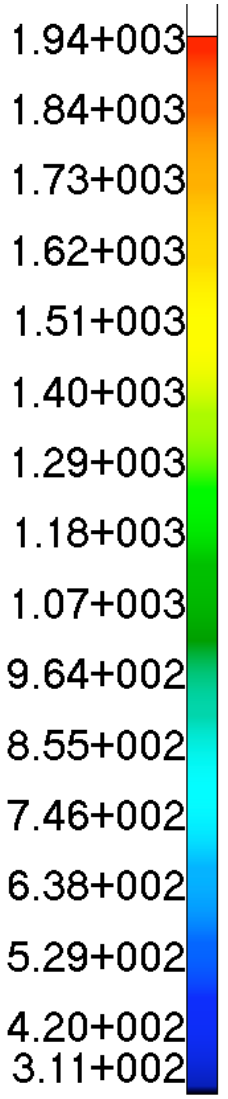

Bottom surface approaches thermal equilibrium faster than top surface

Structural Analysis Results: Displacements

- Thermal loads applied to structure at each time step. Deformation occurs as a result of differential thermal expansion
- Static structural problem solving using Nastran finite element software
- Analysis includes thermal loads only. Working to also apply aero pressures

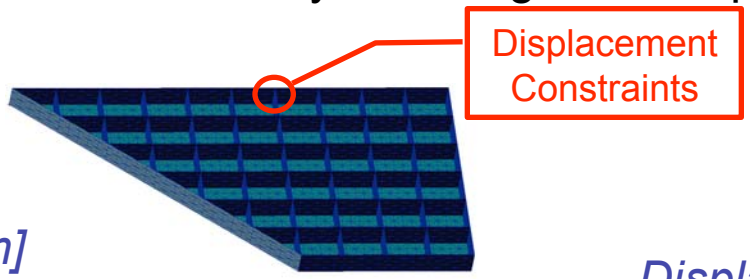

Displacements [m] at 50 s

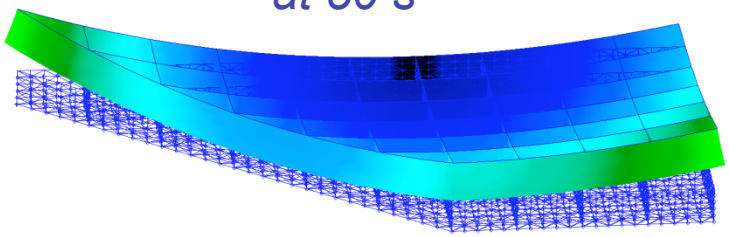

Displacements [m] at 2,000 s

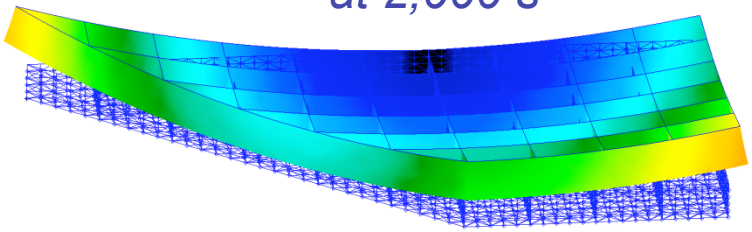

Max displacement increases until bottom surface begins to reach steady state

Displacements [m] at 100 s

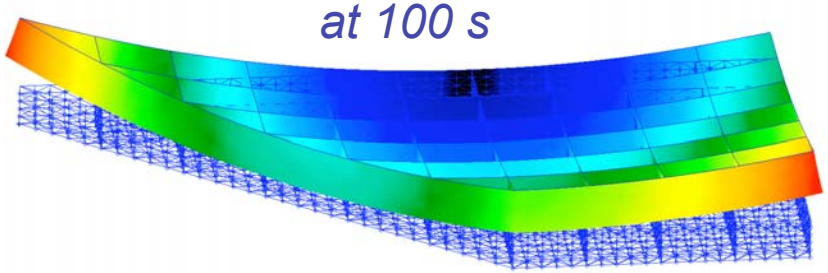

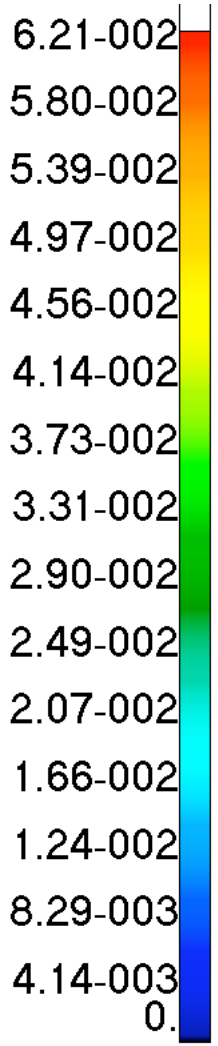

Flow Turn Angle Distribution

- Absolute flow turning angle measured from freestream vector to tangent vector
- Relative turning angle is difference between absolute angle at current and upstream nodes

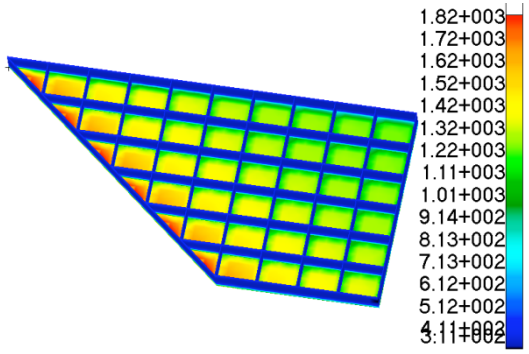

Temperatures [K] at 100 s

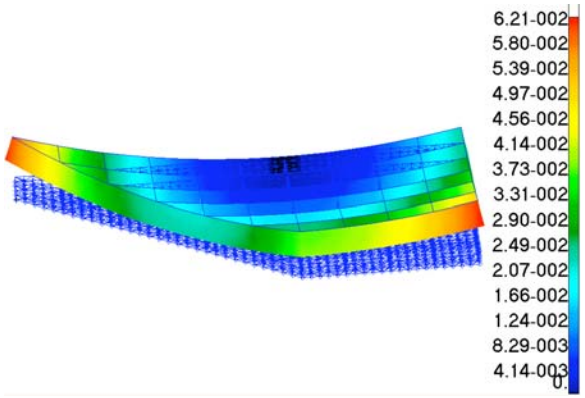

Displacements [m] at 100 s

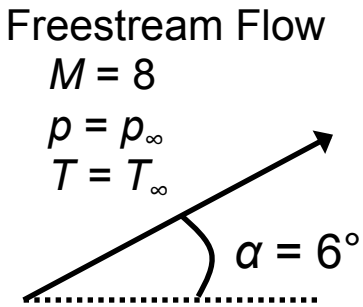

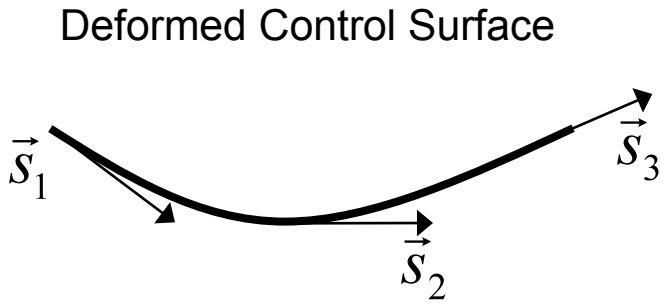

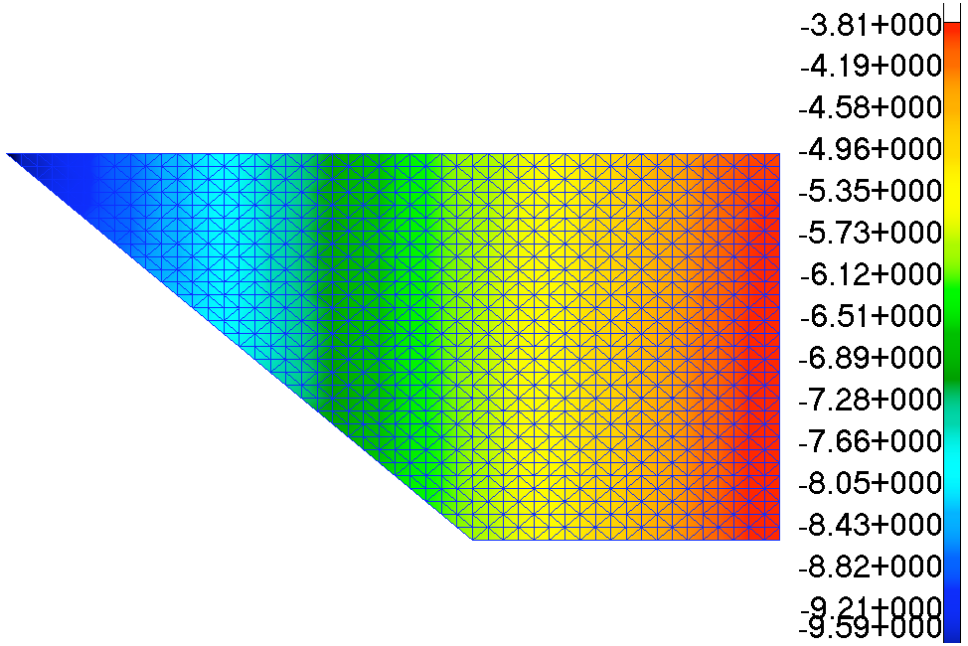

Absolute nodal flow turning angles [degrees] over top skin at 100 s

Aerodynamic Pressure Distributions

- Nodal pressures averaged for each element and pressure treated as uniform over each finite element
- Pressure higher in general on bottom surface than on top surface due to effective angle-of-attack
- Pressure decreases along chord on bottom surface because flow must expand over curved surface after it goes through oblique shock at leading edge
- Pressure increases along chord on top surface because flow is compressed after it goes through expansion fan at leading edge

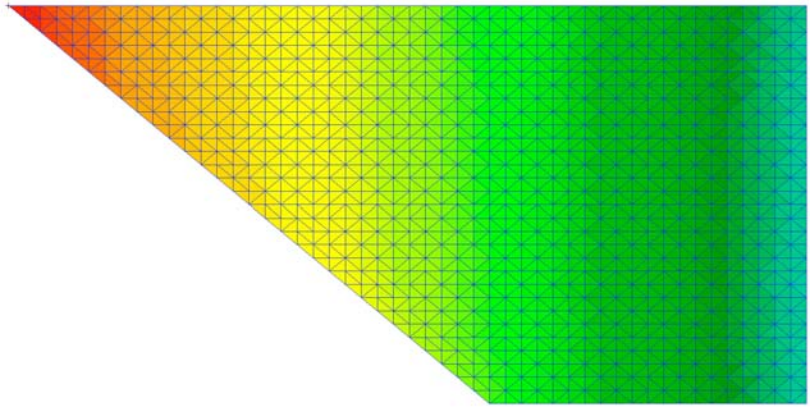

Aerodynamic pressures [Pa] over bottom surface at 100 s

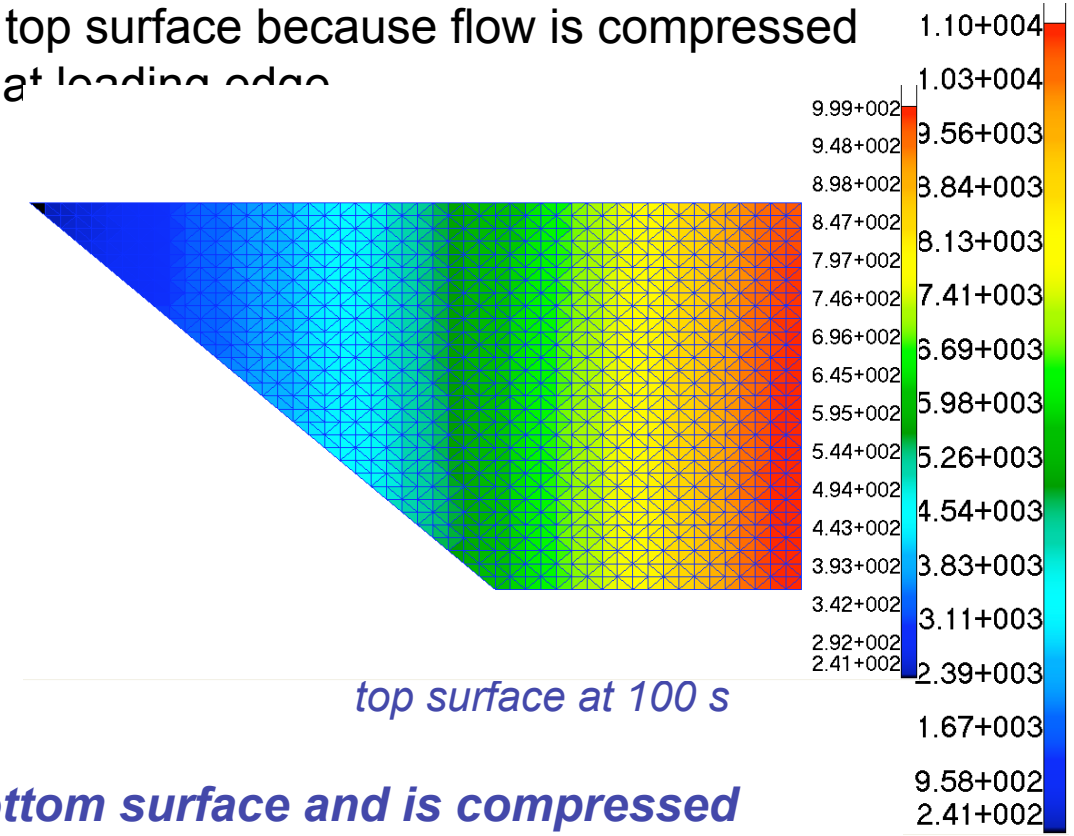

top surface at 100 s

Flow expands over bottom surface and is compressed over top surface due to curvature

Aerodynamic Lift and Drag Forces vs. Time

- Pressure resolved into component parallel to freestream direction for drag and perpendicular to freestream direction for lift
- Skin friction drag computed using skin friction coefficient at Eckert reference conditions. Also includes effect of pressure drag
- Lift decreases up until bottom surface begins to reach thermal equilibrium, then begins increasing; opposite occurs for drag

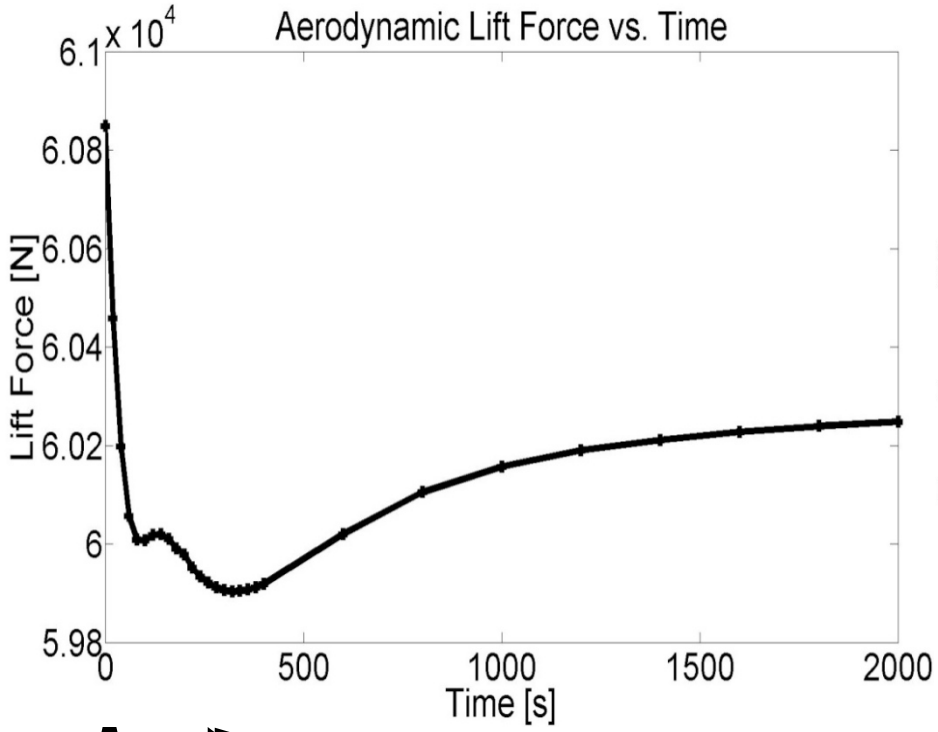

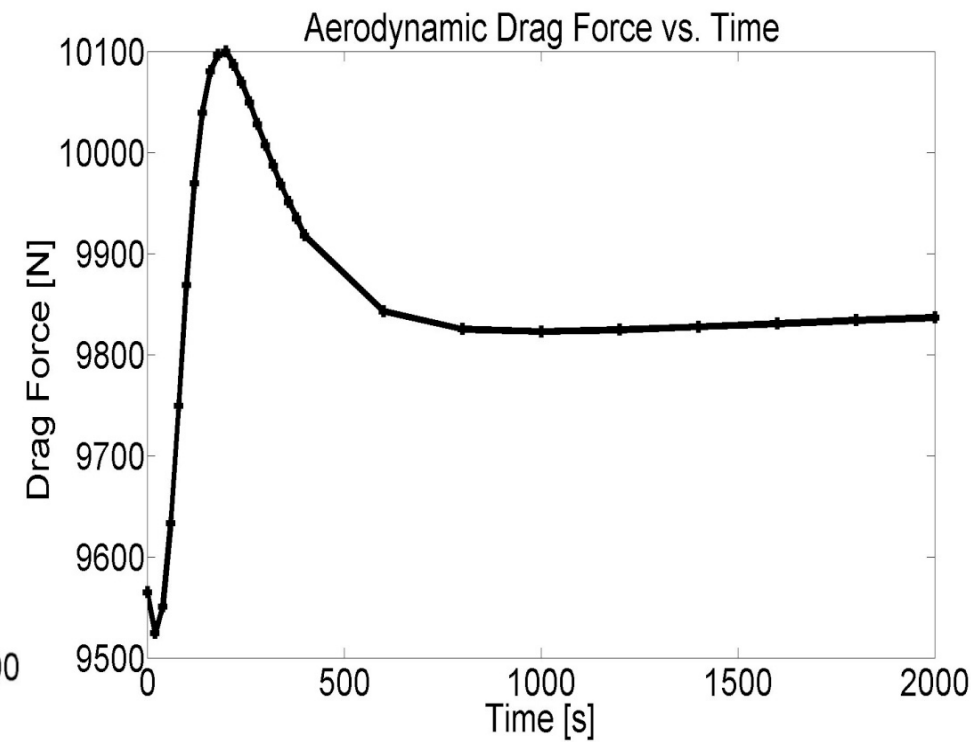

Max relative change in lift is 1.6%

Max relative change in drag is 6.0%

Incorporation of Control System

- Vehicle must be able to account for change in aero forces/moments
- Use control inputs to modify aerodynamic flow and achieve targeted objective
- Aerothermoelastic effects will alter forces and moments acting on vehicle

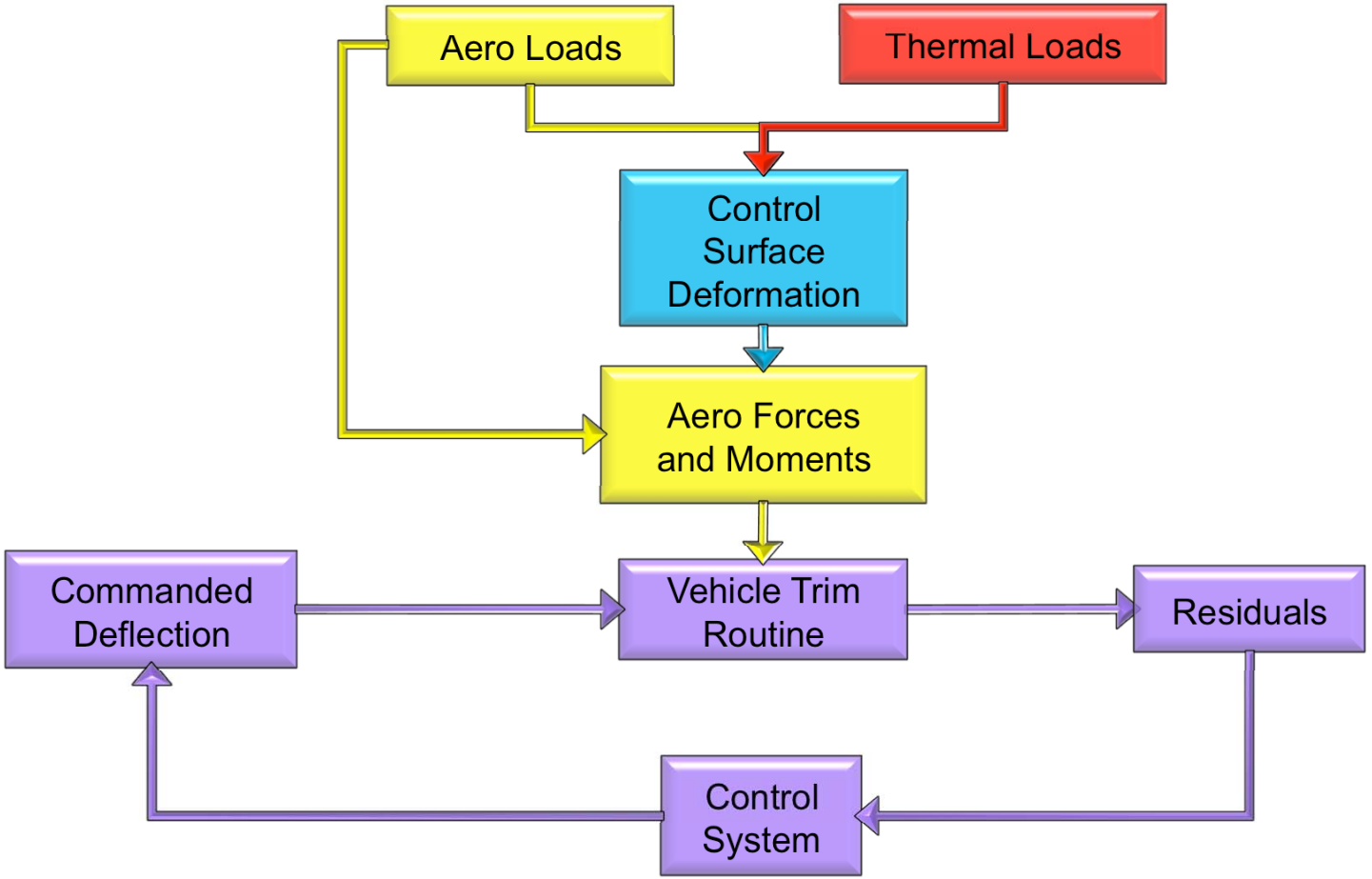

Incorporation of control system will provide insight into control authority required to account for aerothermoelastic effects

Agenda

- Motivation and Problem Overview
- Reduced Order Thermal Modeling
- Reduced Order Structural Dynamic Modeling
- Effect of Structural Deformation on Aerodynamic Forces
- Summary and Future Work

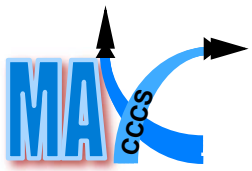

Summary and Future Work

- **Goal**: Create overall computational framework for reduced-order thermoelastic analysis of hypersonic vehicles
- **Major Milestones**
  - Developed framework (to be fully implemented) for reduced-order solution of thermoelastic problem
  - Generated initial results showing effect of thermal stress on natural frequencies
  - Developed framework for 3D quasi-static integrated aerothermoelastic analysis of an HSV control surface
  - Performed study of effect of deformation due to thermal loads on aerodynamic forces

- **Future Work**
  - Currently working to re-design control surface and re-evaluate material selection based on allowable stresses, deflections, and temperatures
  - Incorporate representative heat flux boundary conditions from aeroheating analysis
  - Extend thermal ROM formulation to account for time-dependent boundary conditions, thermal radiation, and temperature-dependent thermal conductivity
  - Couple structural dynamic solution with unsteady aerodynamic formulation and assess effect of aerodynamic loads on structural response
  - Incorporate trim/control routine to assess control input required to account for aerothermoelastic effects

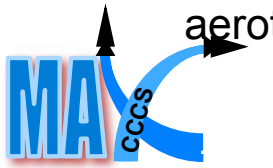

Relevant Publications

- **Published Papers**
  - Falkiewicz, N., and Cesnik, C.E.S., "A Reduced-Order Modeling Framework for Integrated Thermo-Elastic Analysis of Hypersonic Vehicles," *Proceedings of the 50th AIAA/ASME/ASCE/AHS/ASC Structures, Structural Dynamics, and Materials Conference*, May 2009.
  - Falkiewicz, N., Cesnik, C.E.S., Bolender, M., and Doman, D., "Thermoelastic Formulation of a Hypersonic Vehicle Control Surface for Control-Oriented Simulation," *Proceedings of the 2009 Guidance, Navigation, and Control Conference and Exhibit*, August 2009.

- **Planned Papers**
  - Falkiewicz, N., and Cesnik, C.E.S. "Reduced-Order Coupled Aerothermoelastic Analysis of Hypersonic Vehicle Structures," *Proceedings of the 51st AIAA/ASME/ASCE/AHS/ASC Structures Structural Dynamics, and Materials Conference*, April 2010. In progress.
  - 2010 GNC Conference (with McNamara and Crowell, OSU)
  - Journal Submission

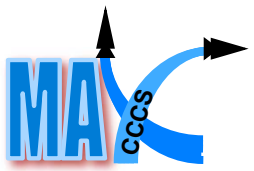

Updated Control Surface Model

Planform and Cross-Sectional Geometry

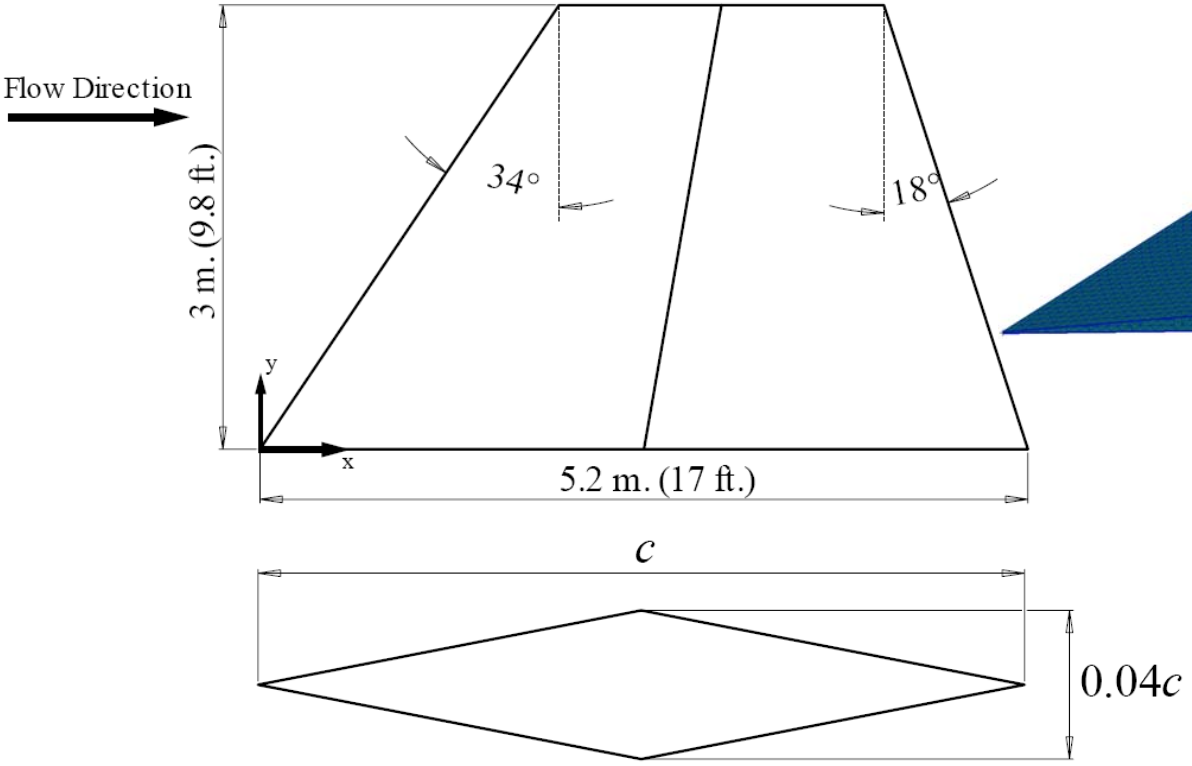

Finite Element Model

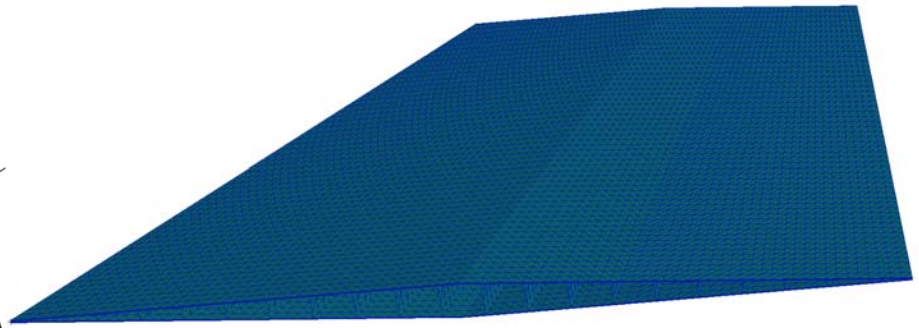

Material Stacking at OML

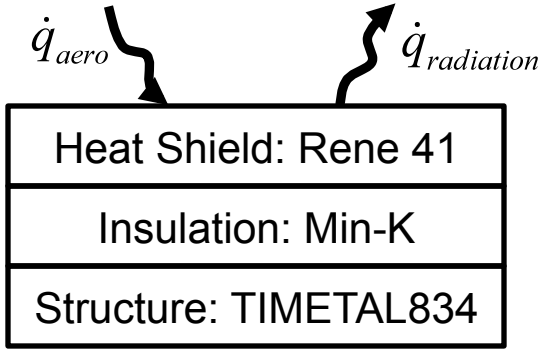

Material Properties Used in Model

	ρ $[kg/m^3]$	E $[Pa]$	ν	α $[\mu m/m/K]$	k $[W/m/K]$	c_p $[J/kg/K]$	T_{max} K
Rene 41	8240	Temp-dependent	0.31	Temp-dependent	18	541	1500
Min-K	256	Neglect	Neglect	Neglect	0.052	858	1250
TIMETAL834	4550	Temp-dependent	0.31	11	7	525	873